CHALMERS

Fatigue Strength of Truck Components in Cast Iron

Fatigue Rig Design, Test Results and Analysis

Master's Thesis in Solid and Fluid Mechanics

ANDERS OLSSON

Department of Applied Mechanics
Division of Dynamics
CHALMERS UNIVERSITY OF TECHNOLOGY
Göteborg, Sweden 2011
Master's Thesis 2011:12

MASTER'S THESIS 2011:12

Fatigue Strength of Truck Components in Cast Iron

Fatigue Rig Design, Test Results and Analysis

Master's Thesis in Solid and Fluid Mechanics

ANDERS OLSSON

Department of Applied Mechanics
Division of Dynamics
CHALMERS UNIVERSITY OF TECHNOLOGY
Göteborg, Sweden 2011

Fatigue Strength of Truck Components in Cast Iron
Fatigue Rig Design, Test Results and Analysis
ANDERS OLSSON

Master's Thesis 2011:12
ISSN 1652-8557
Department of Applied Mechanics
Division of Dynamics
Chalmers University of Technology
SE-412 96 Göteborg
Sweden
Telephone: + 46 (0)31-772 1000

Chalmers Reproservice
Göteborg, Sweden 2011

Fatigue Strength of Truck Components in Cast Iron
Fatigue Rig Design, Test Results and Analysis
Master's Thesis in Solid and Fluid Mechanics
ANDERS OLSSON
Department of Applied Mechanics
Division of Dynamics
Chalmers University of Technology

Abstract

Fatigue properties of a two spherical graphite cast irons, (SGI), EN-GJS-500-14 and EN-GJS-500-7 in an as-cast truck component are evaluated. The examined component is a V-stay anchorage, and has a function of fixating the rear axle of a truck. The component is currently cast in the conventional SGI, EN-GJS-500-7. The matrix of EN-GJS-500-7 consists of a mixture of pearlite and ferrite. The mixture can vary within a component, depending on wall thickness and cooling time, leading to large variations in the hardness of the material. The newer SGI, EN-GJS-500-14, is solution strengthened with silicon and the matrix consists only of ferrite giving the material a more even hardness distribution. Large variation in hardness makes machining hard to optimize, which gives EN-GJS-500-14 an advantage in components requiring machining. To change materials in truck components, fatigue properties of the as-cast component is needed.

The component is tested in a rig, designed so that the component experiences truck-like loading and boundary conditions. The stress response in the component, under truck-like conditions and rig conditions, is computed in FE analyses. Parameters affecting the stress response are identified and their influence evaluated in the analyses.

Due to time limitations the fatigue testing is not completed before the publication of this report. Therefore, no conclusions about the fatigue strength of EN-GJS-500-14 are included in this report.

The main contributions of the thesis are the design of a physical fatigue test rig and an evaluation of parametric influences from FE analyses. The results from the simulations have been used to build a physical rig where V-stay anchorages can be tested under truck-like conditions. Some test results are included in the report, but large parts of the test scheme have, as mentioned, not yet been performed.

Contents

Preface

The work behind this report has been carried out at Volvo 3P in Gothenburg between November 2010 and April 2011 as a part of the solid and fluid master program at Chalmers University.
I would like to take the opportunity to thank the people that have helped me during the course of the work. Firstly I would like to give a special thanks to my supervisor at Volvo 3P Richard Söder for his inexhaustible encouragement and support throughout this master thesis.
I would also like to thank:
My examinator Anders Ekberg at Chalmers University for helpful support and fruitful discussions.
Niklas Köppen at Volvo Materials Technology.
The test engineers and mechanics at Volvo's Cab and Vehicle dynamic strength testing department.
Tapio Rantala, Seppo Paalanen, and Tony Pitkanen at the foundry company Componenta.

Göteborg April 2011
Anders Olsson

1 Introduction

Fatigue is one of the most important parameters to consider when designing truck components. The components are typically subjected to dynamic loads when in service. Many structural truck components are made from spherical graphite cast iron, SGI, and the material is also used in a large number of other applications. The material is popular due to the possibility to form complex geometries without requiring too much machining, in combination with good mechanical properties. The SGI mainly used today is EN-GJS-500-7, here called 500-7, which has been used for many years in the truck industry. It has a matrix consisting of a mixture of pearlite and ferrite surrounding the spheroidal graphite. The pearlite has a strengthening effect, raising the tensile strength of the material but at the same time lowering the ductility compared to a ferritic matrix. The first number in 500-7 represents the tensile strength and the latter the elongation. Some years ago, a new SGI called EN-GJS-500-14, here called 500-14, entered the market, sometimes referred to as being part of the second generation of SGI's. The matrix consists of ferrite surrounding the graphite nodules. Instead of being strengthened by pearlite the matrix is solution-strengthened by silicon. This gives a material with the same tensile strength but with a higher yield strength and a far better ductility. A comparison of the microstructure of the two materials can be seen in figure 1.1.

Components cast in 500-7 usually have large variations in hardness due to varying pearlite/ferrite composition. The composition varies between sections with different thickness and cooling rates during manufacturing. One of the main improvements with 500-14 is that the cast components have a lot lower hardness variations due to that the matrix is fully ferritic throughout the component. This makes it possible to optimize machining. As it seems, it would be possible to switch to 500-14 where 500-7 is used today since testing has shown that the material is as good or better with respect to all essential mechanical parameters, except for wear resistance which is better in 500-7 due to the pearlite content. However, the as-cast fatigue properties of an operational component have not yet been fully examined.

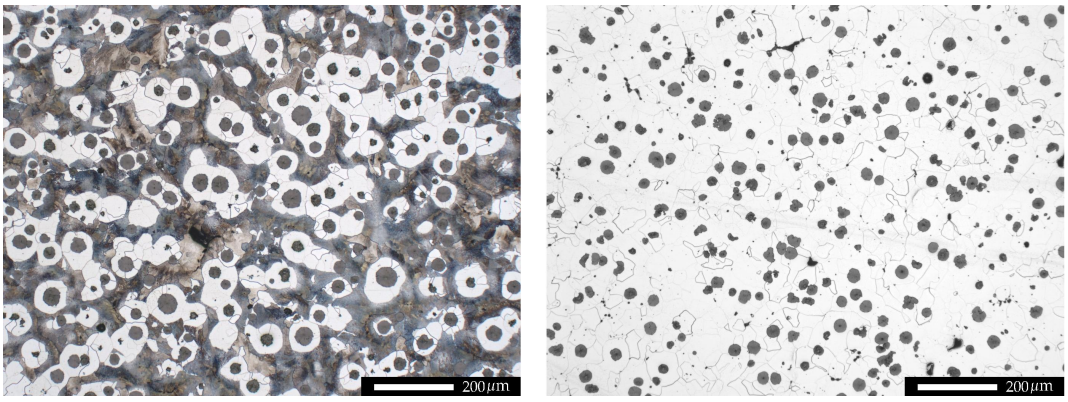

Figure 1.1: Microstructure of 500-7 (left) and 500-14 (right). Nital etched (Volvo Materials Technology)

1.1 Purpose

Materials with better mechanical properties can be used to lower the weight of the components. It is of course of great interest to truck manufacturers, both in order to be able to increase the weight the truck can carry, and to improve fuel efficiency. This has many benefits; some of which are a lower environmental impact, lower cost for customer and a possibility to attain emission standards.

There exist some fatigue data for the two materials from tests performed on standard samples. But in order to switch production to the new material, fatigue data from a real as-cast component is needed. The purpose of this thesis work is to examine the fatigue properties of the 500-14 material and compare it to the 500-7 material on an as-cast component. For the fatigue testing a test rig is needed. It is important that the conditions in the rig resemble those of a real truck in order the make the results as usable as possible. To secure that the stress conditions in the rig do not vary too much from the case in a real truck, finite element analyses need to be performed comparing the two cases.

1.2 Approach

The test component is a typical truck component cast in the 500-7 material and can be seen in figure 1.2. It is called a V-stay anchorage and has the function of fixating a rear axle on a truck. The forces are being transmitted from the rear axle to the V-stay anchorage by the V-stay, seen in figure 1.3. The component is chosen as a test object mainly due to its manageable size and its uncomplicated load case. Since the V-stay is connected to the axle with a ball joint and a rubber bushing to the V-stay anchorage there will practically be no bending moments transmitted.

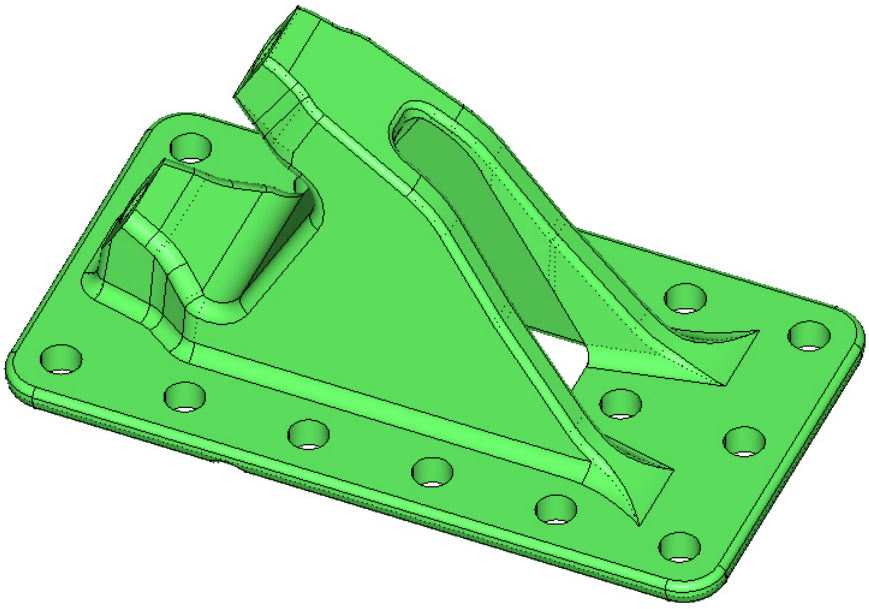

Figure 1.2: Analysed component – V-stay anchorage

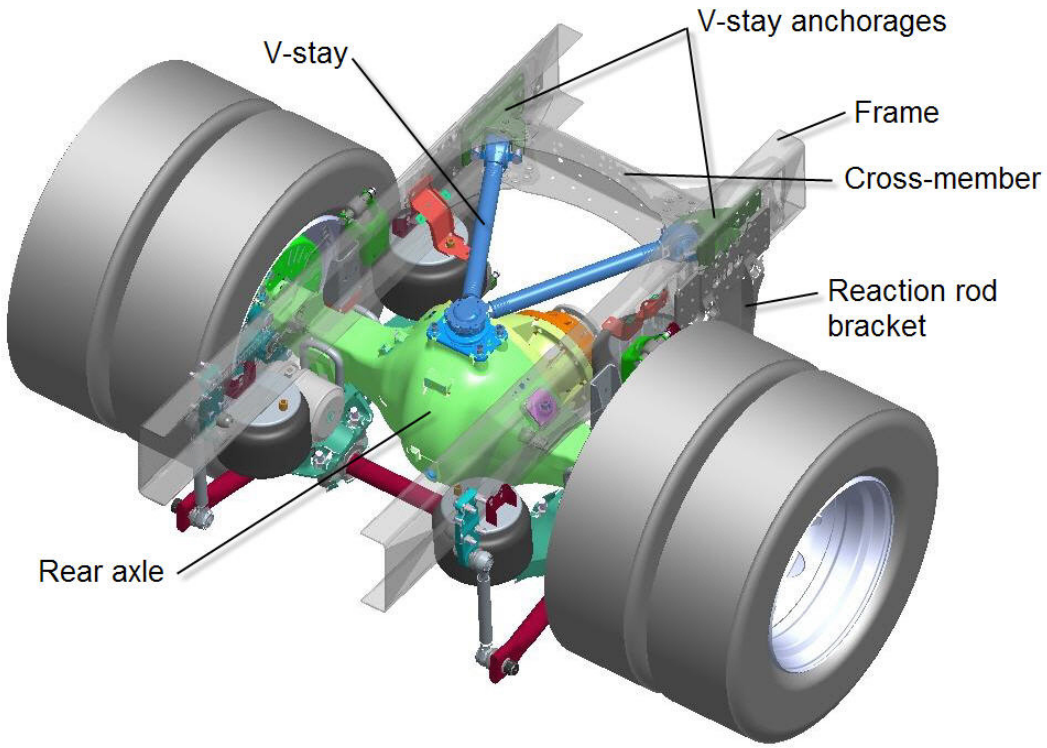

Figure 1.3: Truck frame and axle

To be able to ensure that the stress response in the test rig is reasonable compared to that in an operational truck, a number of FE-analyses need to be performed. As a reference, a model corresponding to a truck will be used. The aim of the FE analyses is to identify parameters affecting the stress field in the V-stay anchorage to be able to build a fatigue test rig with truck-like conditions and to find suitable loading parameters. The examined parameters are listed below.

- Load angle
- Rig length
- Adjacent components
- Fasteners modeling
- Tensile and compressive load
- Fatigue life
- Eigenfrequencies

The test component is cast in two different spheroidal graphite cast irons, 500-7 and 500-14. The fatigue test aims to identify if the solution strengthened SGI, 500-14, is better from a fatigue point of view than the conventional 500-7 material used today.

The aim is to perform tests at two different stress amplitudes, for loads with both constant and variable amplitudes, to be able to estimate Wöhler-curves for each of the two materials. Achieving truck-like conditions in the rig is not crucial for the comparing tests performed in this thesis. However, the rig is to be used also by other projects were absolute testing is performed. It is therefore important that the stress response in the V-stay anchorage is similar to operational loading in trucks.

1.3 Limitations

Due to time limitations the complete test program will not be completed before the publishing of this report. The remaining tests will be performed by Volvo following a scheme set up by the thesis worker.

2 Theory

2.1 Material

Cast iron is a class of ferrous alloys with a carbon content above 2.14 wt%. In production the carbon content is often between 3.0-4.5 wt% [3] since this is around the concentration that minimizes the melting temperature. Actual minimum is called the eutectic point and is around 4.2 wt% with a melting temperature, around 1150° C, which makes them suitable for casting. In gray cast iron the graphite takes the form of flakes surrounded by a ferrite and/or pearlite matrix. Since the flakes work as severe stress raisers the material is comparatively weak and brittle in tension.

In SGI, small amounts of magnesium and/or cerium is added to the melt before casting. This causes the graphite to form as sphere-like particles called nodules. The spherical shape of the nodules is very beneficial for the mechanical properties of the material. The result is a material with far better yield strength, tensile strength and ductility than gray iron, sometimes with properties close to steel.

Small deviations from the correct processing procedure may introduce several types of defects into the material. Basic quality parameters for spheroidal graphite cast iron are e.g. macrohardness, graphite nodule shape, surface roughness and amount of casting defects, [9].

2.1.1 Matrix structure

In FE analysis, cast iron is usually treated as an isotropic material even though it is a composite material consisting of graphite nodules and a matrix structure consisting of ferrite and/or pearlite. Both it's mechanical and fatigue properties are controlled by its microstructural characteristics, [4]. Ferrite normally has fairly low strength and high ductility compared to the strengthening pearlite which has a high strength but is fairly brittle. The ratio between ferrite and pearlite in the material is set to achieve the desired properties. Instead of having pearlite as strengthener, the 500-14 material is solution strengthened by silicon.

Silicon is a material that will interact with the graphite formation and affect the resulting microstructure and is therefore included in the formula for the Carbon Equivalent, CE. The CE is usually defined as:

$CE=C+(Si+P)/3$

The CE can be used to determine if the iron is over, under, or at the eutectic point at 4.26 wt%.

2.1.2 Graphite structure

The shape of the nodules does of course also affect the mechanical properties of the material. The optimal nodule shape is spherical but some graphite may be formed in a deteriorated shape. The nodularity rating is a way to describe the quality of the nodules, where 100 % means that all nodules are completely round. A common requirement is that a 80–90 % nodularity is reached. A high nodularity is beneficial from a fatigue point of view, since degenerated graphite work as stress raisers where cracks may initiate, [8].

The nodule count is usually defined as the number of graphite particles per square millimeter. A high nodule count corresponds to an overall fine grained microstructure which gives better mechanical properties than those with a low nodule count. The nodule count can vary depending on the wall thickness and the cooling rate. Small nodules are beneficial for the mechanical properties, but nodules smaller than 20, 30 μm does not seem to give any additional benefits, [4].

2.1.3 First Generation of SGI's

The 500-7 material belongs to the so called "first generation" of SGI's. It has become popular due to its excellent castability in combination with good mechanical properties. The spheroidal shape of the graphite makes the composition of the harder pearlite and the softer ferrite matrix deterministic for its mechanical properties. This differs from gray irons where the graphite is in the form of flakes and almost fully determines the ductility, almost unaffected by the pearlite-ferrite composition. The matrix composition in SGI's can be controlled by adjusting the chemical composition to range from fully ferritic to fully pearlitic. SGI's with a mainly ferritic matrix shows a higher ductility but lower strength than SGI's with a mainly pearlitic matrix.

A clear way to see how the matrix composition affects the mechanical properties is to compare the dominantly ferritic material EN-GJS-400-18 to the dominantly pearlitic material EN-GJS-700-2, [15]. As their names reveal the tensile strength increases from 400 to 700 MPa and the ductility decreases from 18 % to 2 %, going from a ferritic to a pearlitic dominated matrix. At the same time the hardness increases from 155 ± 25 HBW to 265 ± 40 HBW mainly due to the pearlite content.

The main drawback of the first generation of SGI's is that the composition of pearlite and ferrite is sensitive to the local cooling rate and to variations in the amount of pearlite-stabilizing elements, e.g. manganese, copper and tin. This leads to variations in hardness, strength and ductility within a component, but also within and between different batches. The large hardness variation makes machining troublesome since the operations are difficult to optimize.

2.1.4 Second Generation of SGI's

The fully ferritic matrix of the 500-14 material has a high amount, 3.7-3.8 wt%, of silicon added to it, compared to 500-7 where the silicon level is 1.5-2.8 wt%. The silicon fills the function of strengthener instead of pearlite and does not have the same negative influence on the ductility. Owing to this, the ferrite in the 500-14 material is about 70 % stronger than the ferrite in 500-7, [13]. This gives a material with the same tensile strength as 500-7 but with a higher ductility. The main benefit is however the reduced scatter in hardness making machining easier to optimize. It has been shown that a conservative estimation of the theoretically possible cost reduction is 10 % together with a 5-20 % time reduction, [2]. The main reason for the improved machinability is the ferritic single-phase matrix consisting only of ferrite which makes the hardness variations small. The hardness variations in the 500-14 material is said to fall within an as narrow band as ± 15 HBW in operational components as long as the variations in silicon content is kept

within 0.1 wt%, [12]. The scatter is said to usually be even less, as small as 5–10 HBW . In the proposed EN standard, PrEN 1563:2009, [15], the Brinell hardness range is 185–215 HBW for a relevant wall thickness below 60mm. This should be compared to the 150–230 HBW for the 500-7 material. In [2], two operational components are cast in both the 500-7 and the 500-14 material and the hardness is measured. The hardness variations are shown to be reduced from ±24 to ±4 HBW, and it is concluded that this is due to the single-phase ferritic matrix.

The production cost of the V-stay anchorage is dominated by the cost at the foundry e.g. material. Only 6 % of the total cost is related to machining. This means that the component is not optimal for lowering the total cost by better machining properties. The savings in machining cost for the V-stay anchorage is estimated to be 6-8 %, leading to a 1-1.5 % lower total cost, [16]. The estimated increase in machining speed is 10-15 %. The lowering of the total cost would of course be larger in a component requiring more machining.

There are some misconceptions about solution strengthened SGI's dating back to 1949 and a work performed by Millis et al [7] where it was stated that an increase of silicon above 2.5 wt% lowered the mechanical properties especially toughness, tensile strength and/or ductility. All of the tested alloys containing more than 2.5 wt% silicon did however also contain more than 0.8 wt% manganese which is stabilizing pearlite. This would give a matrix of solution strengthened brittle pearlite instead of ductile ferrite explaining why SGI's with high silicon content was avoided. Silicon does reduce the ductility of the material from around 20 % at a content of 2.25 wt% to around 16 % at 4 wt%, however, the ductility is still much higher in 500-14 than in 500-7, [2].

2.1.5 Mechanical properties

A comparison between the most important mechanical properties of the 500-7 and the 500-14 material can be seen in table 2.1 and table 2.2. The hardness is presented for two ranges of relevant wall thicknesses, t. The data are from separately cast test bars. The actual mechanical properties in operational components can be lower and varies between sections with different thicknesses.

Table 2.1: Mechanical properties, [15]

	Minimum yield limit [MPa]	Minimum tensile strength [MPa]	Elongation [%]	Hardness [HBW] $t \leq 60$ mm	Hardness [HBW] $60 < t \leq 200$ mm
500-7	300	480	7	170-230	150-230
500-14	400	480	14	185-215	170-200

Table 2.2: Fatigue properties, [15]

	Fatigue limit [MPa] (rotating bending) unnotched	Fatigue limit [MPa] (rotating bending) notched	Fracture toughness [MPa$\sqrt{\text{m}}$]
500-7	224	134	22-25
500-14	225	140	28

As seen in table 2.2, the fatigue properties of the 500-14 does not seem to be significantly better than the 500-7 material, but should be at least as good.

2.1.6 Test results from manufacturer

Fatigue testing of standard samples has been performed at the manufacturer Componenta, simultaneously as the testing at Volvo. The samples in 500-14 are cast from the same batch as the V-stay anchorages and are tested under rotating bending. The testing is not yet completed but preliminary results suggest that the fatigue strength of 500-14 in standard samples does not seem to be better than for 500-7.

2.1.7 Defects

Casting defects is a generic term for unintended deviations in the material, such as inclusions of slag or sand, shrinkages, mould erosion, gas blisters etc. The cast material has a non-homogenous microstructure with slightly varying properties. In [13], it is concluded that the fatigue characteristics of a cast material is governed by the defect level. Metallurgical defects in SGI can also be very costly for the foundry since the component needs to be scrapped, but also because they sometimes are not found until after the expensive machining stage. To be able to limit the defect level in the final component it is important to select raw material with care and to have control over the process. Defects are also of great importance since they work as initiation sites for fatigue cracks. The defect level is strongly connected to the casting process. In structural truck components the highest stress is typically at the surface which makes defects there most important from a fatigue point of view. There are a number of defects that may be present in cast iron, the most important are explained below.

Porosity There are two main reasons behind porosities in the cast material: dissolved gases in the melt and shrinkage pores, [10]. Gas porosity can be caused by gases trapped in the mould during filling or by gas released as the solubility decreases during cooling. Shrinkage pores are formed as the cast component solidifies and the material contracts. If the feeding system fails to provide new material it will cause shrinkage. If the contraction is restricted, tensile stresses and/or pores will occur in the material which in some cases may cause the component to break under processing. Microporosities are shown to be the most likely site for crack initiation compared to other defects, [13]. Shrinkage can also make it hard to fulfill the dimensional tolerance requirements.

Roughly, 50 % of shrinkage defects are related to sand systems, feeding and gating and the other 50 % are related to metallurgical factors such as carbon equivalent, temperature, inoculation or high magnesium residuals, [6].

Inclusions Inclusions may be formed through oxidation of the melt or by intermetallic reactions. The main reasons for such defects are incorrect holding time or holding temperature [9]. Non-metallic inclusions can come from slag, molding sand or a binder that has been introduced to the melt during the process. The size of inclusions vary but is ranging from roughly 5 μm up to several millimeters. Since slags are lighter than the metal they often end up as surface defects, providing a typical crack initiation site.

Degenerated graphite In some cases the graphite is not formed as spherical nodules but instead in a degenerated form. Generally two different types can be distinguished between; large unspherical graphite and chunky graphite. Inside the component degenerated graphite can also be present due to improper casting conditions, foundry malpractice or low quality raw material. The main factor affecting degenerated graphite is the solidification time, which causes it to be more common in the thermal center of thicker casting sections. The most common cause of chunky graphite formation is an excessive concentration of rare earths and a high carbon equivalent. There is however also evidence that chunky graphite may be related to low oxygen concentration [11]. When comparing the fatigue properties of a material containing chunky graphite with data used in the industry it is concluded that chunky graphite is roughly equally dangerous as an as-cast surface, [1].

Surface defects Cast components normally have a rugged surface suffering from various irregularities. This is of course not beneficial from a fatigue point of view since the irregularities work as stress raisers enabling cracks to initiate.

At the surface of the cast components there can exist deteriorated graphite that may be due to metal-mould reactions and decarburizing in the just solidified metal. According to [1], high silicon ferritic irons do not experience decarburization at the cast surface.

The machining of a component might cause micro flaws in the material that can be an initiation site for a fatigue crack. It has been shown that a spheroidal graphite cast iron with a ferritic matrix is not prone to form crack initiation sites during machining, [1].

2.2 Fatigue

Mechanical fatigue is a form of failure that occurs when a material is subjected to repeated loading. The component may fail even if the stress level is well below the yield strength of the material. Fatigue is estimated to cause as much as 90 % of all metallic failures, [3].

Prevention of fatigue failure is one of the most important parameters to consider when designing truck components. The components are typically subjected to dynamic loads when in service. If the stress in a local area exceeds a certain threshold called the fatigue limit, the material will sustain

fatigue damage. If the loading continues long enough a crack will form, which will grow in to the material. The crack will reduce the area that carries load which means that the stress will increase for a given load. When the remaining area is too small to carry the load, final rupture will occur and the component will fail. Since there often is no significant plastic deformation at failure the material response is often like that of a brittle material, even if the material is intrinsically ductile. Due to this brittle behavior there is often no warning, except crack growth, before failure and the failure can be very swift.

A problem with designing against fatigue is that there is a statistical spread both in the load and the strength of a component, as indicated in figure 2.1. Failure will occur in the over-lapping area which corresponds to a high load being applied to a weak component. To be sure of avoiding failure in all cases the two curves need to be separated. This would mean an expensive and heavy component that in almost all cases would be over-dimensioned.

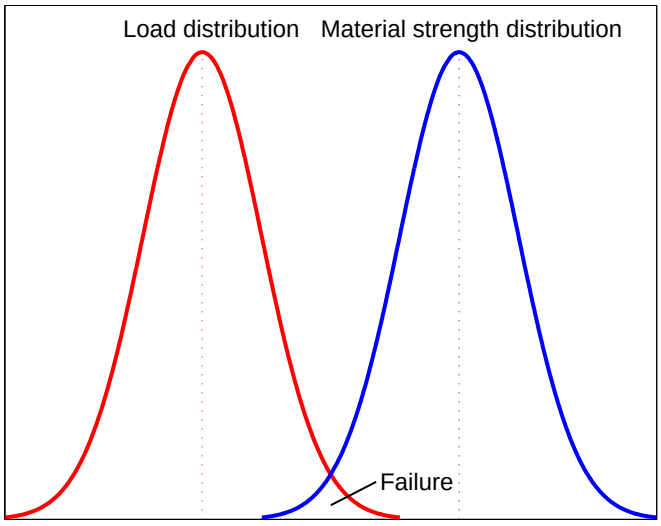

Figure 2.1: Distribution of load and material strength

The failure rate is a trade-off that needs to be made depending on the seriousness of failure. The aim of product development is often to increase a products capacity, which usually means that the load is increased. To avoid an increase in failure rates, a corresponding increase in material, (or rather component) strength is needed.

2.2.1 S–N curve

Fatigue tests are usually performed with standardized procedures and test specimens at several stress levels. If the number of cycles to failure is plotted against stress amplitude in a log–log diagram the data is often found to fall along a straight line. The line is called an S–N curve and if the line is drawn through the center of the data the curve represents a 50 % failure rate. Since a 50 % failure rate is too high in many cases the curve can be shifted to represent a lower failure rate, e.g. 1 %. The S–N curve is a convenient way to find an allowed stress level for a given number of cycles

the component needs to endure. The procedure is therefore widely adopted. However, there is large scatter in the data from machined standard samples, and the scatter amongst and between operational components is even larger. It is therefore obvious that component design is far more complex than what can be included in an S–N curve derived from test specimens. It does however provide guidance to assure reasonable stress levels and should work well to compare fatigue properties of different materials.

By studying the S–N curve in figure 2.2 it is easy to understand why the stress in the test component needs to be thoroughly examined. If the stress in the model is calculated to 150 MPa but in reality is 200 MPa, the fatigue life will be decrease to 25 %, from 1.8e6 to 4.5e5 cycles.

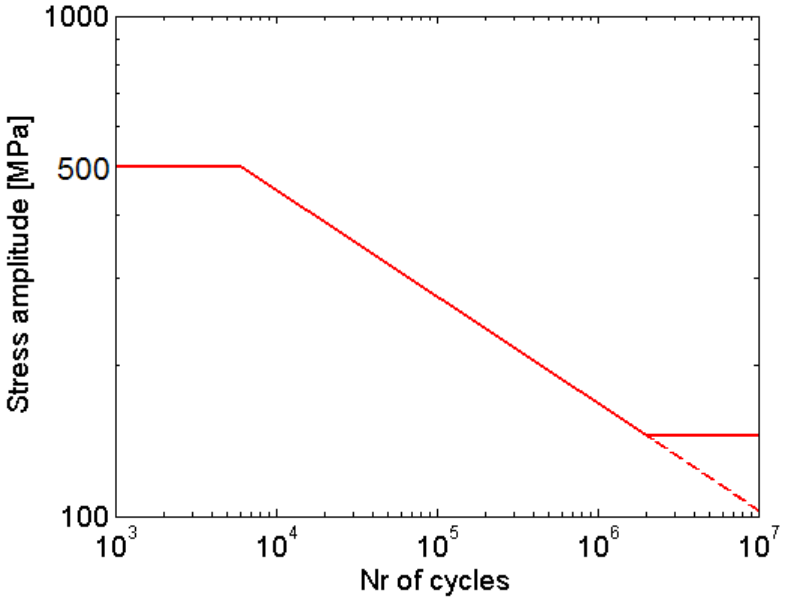

Figure 2.2: S–N curve for as-cast 500-7, recreated from data in [14], 50 % failure rate

2.2.2 Cumulative fatigue damage – Palmgren–Miner rule

A common way to add damage from cycles of different stress amplitudes is to use the Palmgren–Miner rule. The rule states that fatigue damage can be added linearly. For each stress amplitude the ratio between the applied number of cycles, n_i, and the number of cycles to failure, N_f, is calculated and added. The rule states that the component will fail as the accumulated damage, C, reaches 1. Though Palmgrens–Miner's rule is convenient to use and is widely accepted in industry it has limitations. Experimentally C has been shown to range from well below to well above 1. In a random loading case the sequence of the stress peaks will influence the fatigue life. For example a stress peak can give rise to a plastically deformed area with compressive stresses at the tip of an existing fatigue crack and thereby lower crack growth rates. This will give conservative life estimations, but if cycles with low stress amplitude follow upon a cycle with high stress amplitude the crack may propagate even if the fatigue limit is not exceeded for the low stress amplitudes. To compensate for this non-conservative behavior it is common to (theoretically) remove the fatigue limit and just extrapolate the S–N curve below the fatigue limit, as suggested by the dashed line in

figure 2.2.

2.2.3 Cycle Counting – the Rainflow Method

When the load signal is stochastic it needs to be processed in order to enable a calculation of the fatigue life with the Palmgren–Miner rule. This can be done using the Rainflow method which extracts distinct load cycles with given amplitudes and mean stresses. The procedure is explained much more extensively, e.g., in [5].

2.3 Rig design

The construction of the test rig is based on the simple principle that the tested component should experience the same stress distribution as when mounted in a real truck. Since there are many parameters affecting the stress field the aim is to be within ± 10 % of calculated operational stress magnitudes. The rig construction is of course restricted due to a number of practical reasons e.g. the appointed test space, the size of the hydraulic cylinder, stiffness requirements and the possibility to attach the rig firmly to the ground.

2.3.1 Load

The V-stay consists of a right and a left arm each connected to a V-stay anchorage as seen in figure 2.3. The V-stay anchorages in a truck are mainly taking forces that arise when the truck is turning. When studying the load signal measured at the testing ground it can be concluded that the load on the right side is inverted to that of the left side. This means that when the right anchorage is loaded in compression the left one is loaded in tension. This unsymmetrical loading means that the FE model can not be simplified by just modeling one side of the truck. The loading in the rig differs from the truck-like case but is actually also unsymmetrical, see figure 2.3. Mirroring boundary conditions at center-line of the model would reflect the applied force to fall in the shape of a v, instead of falling along a line as the hydraulic cylinder. Since the distances from the anchorages to the center-lines in both models are fairly large it is not expected that the stress field is severely affected even if symmetry is assumed. But, since the computational demands are moderate, the practical benefit of a smaller model would not be that large. Hence, in all calculations on the truck and the rig covered in this report both left and right sides have been modeled.

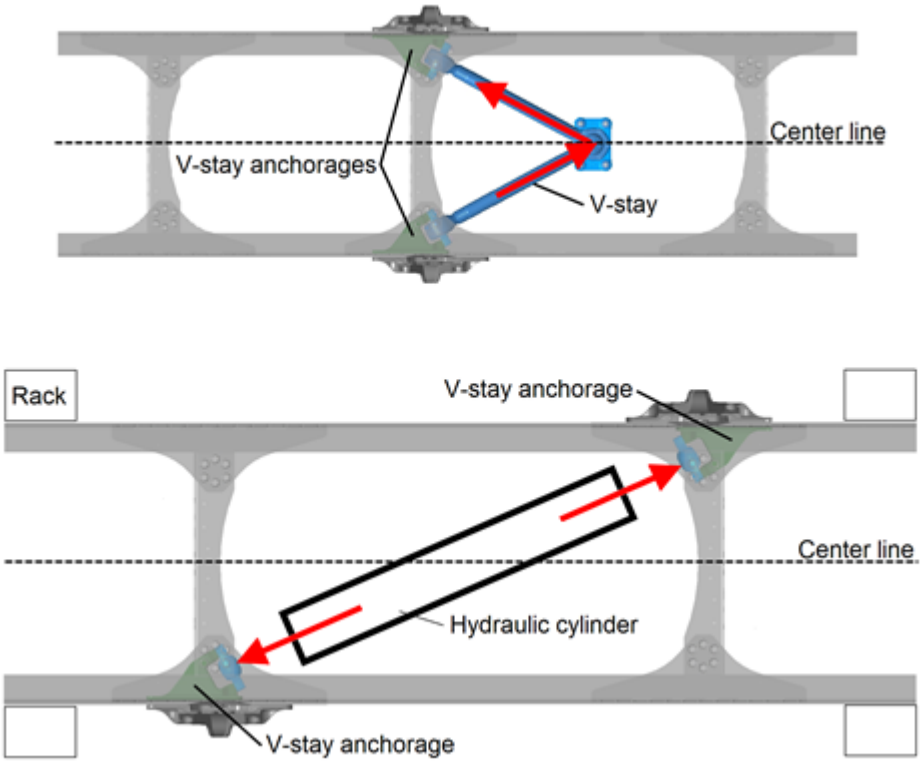

Figure 2.3: Difference between load case in truck (upper) and rig (lower)

It is of course beneficial if the load can be driven with an as high frequency as possible to shorten the test time for each sample. The frequency is however limited due to a number of reasons. The rig needs to be stiff enough so that no eigenmode is excited. The noise level in the test room needs to be limited in order to provide a decent working environment. It is hard to estimate in advance how the noise level is influenced by the load frequency, which means that the frequency might need to be adjusted during the testing until a reasonable noise level is achieved. Tentatively, a reasonable frequency of the load signal is assumed to be around one Hz.

In metallic materials the frequency of the load signal does not affect the fatigue life significantly. Neither does the shape of the load signal, meaning that the signal can be e.g. sinusoidal, square or triangular. In viscous materials such as rubber, the frequency of the load signal is critical since the material properties may change with an increase of temperature induced by the viscous damping. This means that viscous materials are avoided in the rig design and that the rubber bushing connecting the V-stay to the anchorage is replaced with a specially designed component in steel.

3 Method

A number of parameters influencing the stress response in the V-stay anchorage are examined. To be able design a fatigue test rig where components could be tested under truck-like loading and boundary conditions, the following parameters have been identified.

- Load angle
- Rig length
- Adjacent components

The component's fatigue life in testing are to be plotted against the stress amplitudes in the component. Therefore, it is important that the simulations are performed on a model where the resulting stress levels are as reliable as possible. To achieve this, the following parameters are identified and examined.

- Modeling of fasteners
- Compressive vs. tensile load

The loading in the fatigue test needs to be specified in terms of load frequency and magnitude. In order to find suitable values for this, the following parameters are examined.

- Fatigue life
- Eigenfrequencies

3.1 Finite element analysis

For the finite element analysis, FEA, Altair Hypermesh was used as preprocessor. The geometries were imported from ProE files. From Hypermesh an output file was generated and MD Nastran was used as the solver. Postprocessing was performed in Altair Hyperview. The fatigue life estimations were done in LMS Falancs and in Matlab.

The V-stay anchorages and the reaction rod brackets are made out of cast iron and their Young's modulus is set to 165 GPa and Poisson's ratio to 0.27. All other components are made out of steel and their Young's modulus is set to 210 GPa and Poisson's ratio to 0.3.

3.1.1 Mesh

The mesh on the V-stay anchorage was generated in Hypermesh using triangular elements of the first order. When the meshing was completed and optimized the elements were changed to second order elements. This means that the geometry was only captured with flat triangulars but that the simulations were performed on elements with a mid-side node. Simulations were performed with a 3mm representative element size to capture the geometry sufficiently. The initial mesh was generated as a 2D-mesh on the component surfaces. From the 2D-mesh a 3D-mesh was created. Thus, the 3D-mesh consist of second order tetrahedron elements. The simulations featured the

combined 2D/3D-mesh. The 3D-mesh gave the structure its stiffness and the 2D-mesh made it possible to evaluate stress magnitudes at the surface of the component. The 2D-mesh was given a thickness of 0.01mm in order not to increase the stiffness of the component.

The mesh for the V-stay anchorage and the complete truck model and rig model mesh can be found in appendix B.

3.1.2 Boundary conditions

In order to restrict the motions of the model in space, boundary conditions, (BC), are needed. A commonly used BC is to keep some, or all, degrees of freedom, (dof), in a node fixed. There are six dof's in each node where dof 1–3 correspond to translative motions and dof 4–6 correspond to rotations. The boundary conditions used in the simulations restrict all six dof's in selected nodes. The selected nodes are situated at the end of the frame in the truck-like model and at the bottom of the fixating racks in the rig model. A more detailed view of the BC's can be seen in appendix B.

3.1.3 Load angle

The actual loading angle in the truck is given by the angle of the V-stay, see figure 3.1, and is 28.2°. The length of the provided hydraulic cylinder is around 1600mm including load cell and brackets. The rig is built from a truck frame and with two truck cross-members. Measures are given in the sketch in figure 3.1. Since the hydraulic cylinder is 1600 mm it means that the load angle in the rig would be $\arcsin(625/1600) = 23°$. Since this deviates from the real angle of 28.2° it makes it necessary to examine if the stress response is altered significantly.

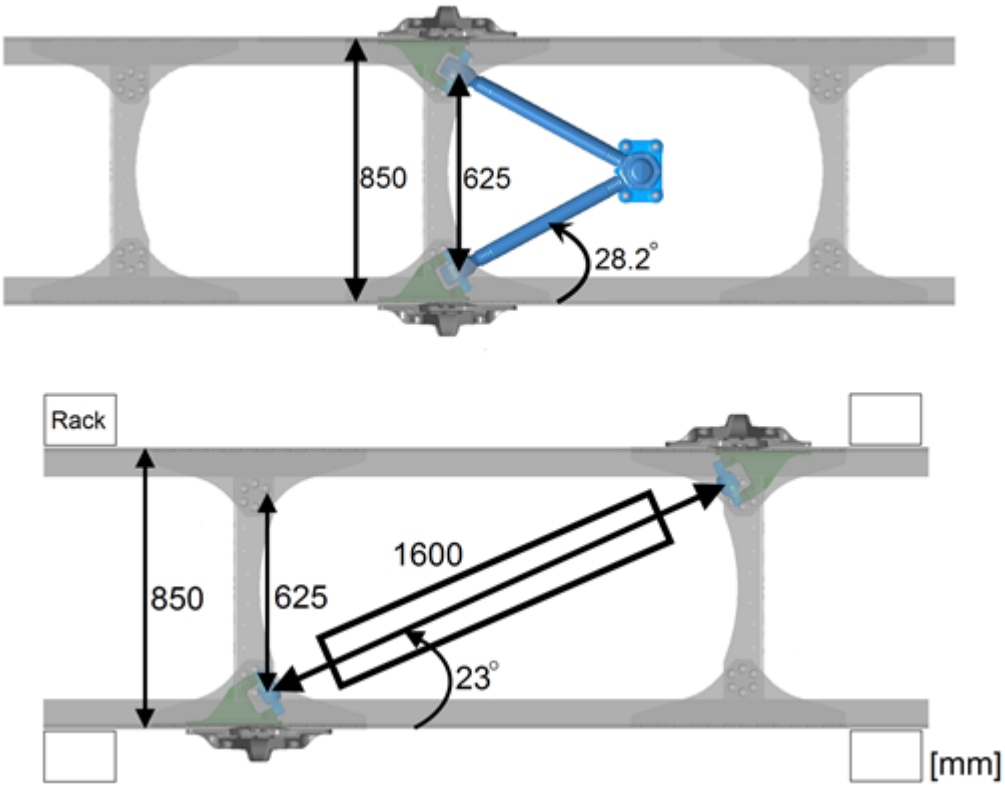

Figure 3.1: Truck-like sketch (upper) rig sketch with unmodified cross-member (lower)

In the FE simulations a unit load of 100 kN load is applied to the bushing connected to the V-stay anchorage. The load corresponds to the forces transmitted by the V-stay in a operational truck. The magnitude of the load in the FE-analysis is of little importance; since the stress response is linear it can just be scaled for any given load.

3.1.4 Rig length

If the rig can be kept short then it is possible to mount it to a vertical wall which would be beneficial since the floor space needed would be greatly reduced. It is assumed that if the V-stay anchorage is mounted too close to the very stiff rack it will greatly affect the stress field. The rig is modeled to be 3 m, since this is the height of the vertical wall. To examine the influence from the rig length, simulations with a 4m model are used as comparison. In the 4m model the distance between the V-stay anchorages and the racks are increased, compared to the 3 m model. However, the distances between the cross-members are kept as in the 3m rig, i.e. the length of the hydraulic cylinder is the same.

3.1.5 Modeling of fasteners

The rig is joined together with rivets and bolts in the same configuration as in a real truck. Generally rivets are used in places where shear forces dominate and bolts are used where axial forces dominate. In the ideal case, rivets are thought of as to only transmit shear forces, but they can of course

transmit some axial load as well. Bolts sustain mostly axial load but the friction between the clamped parts can sustain some shear forces.

In the FE model the bolts and rivets are modeled as seen in figure 3.2. The component's hole edges are connected with rigid stars to the bar-elements, which are all 14mm in diameter. In the idealized case a bolt may only be loaded axially. Hence only the local dof 1 is configured to sustain load and all other dof's are released. In the case of the rivets, the local dof's 2 and 3 are configured to take load, corresponding to shear, whilst all other dof's are released.

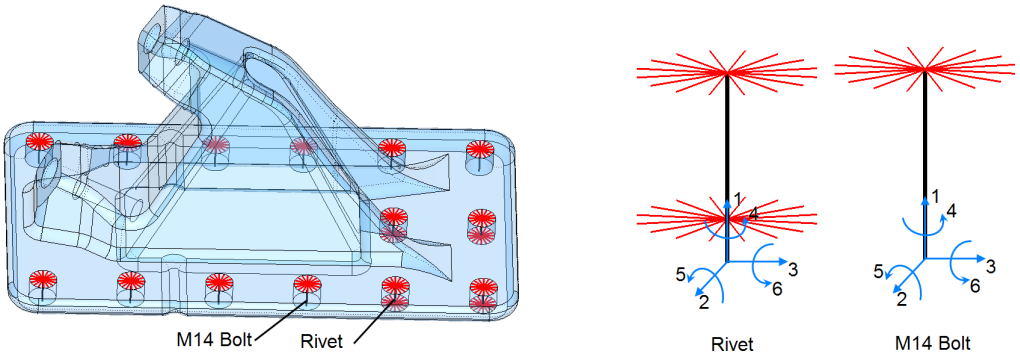

Figure 3.2: Modeling of fasteners – Overview (left), local dof's (right)

The idealized case tends to be a bit too conservative since the component is freer to deform giving rise to higher stresses in the material. Since the aim is to get as close to the correct situation as possible, an alternative method for fastener modeling is used for comparison. In the alternative model, additional elements are created in the same places as the 14 mm bars, but are assigned diameters that are smaller than 14 mm. The additional elements are allowed to take only shear forces in the case of a bolt and only axial load in the case of a rivet. In a real joint, both bolts and rivets can be loaded axially and in shear which means that this model hopefully will mimic a more realistic case. A rivet is assumed to take a few kN axially and the bolts are assumed to take shear forces corresponding to the clamping force after settling plus additional external axial loading times the friction coefficient. This results in an allowed shear force for the bolts that is approximately 5 kN. The reaction forces in the additional elements are extracted from the solver and the diameter of the bars are redefined until reasonable forces are obtained.

3.1.6 Compressive vs. tensile load

In an attempt to make a model as close to the real situation as possible two models where made, one for the case of compression and another in the case of tension. In both cases the bolts are allowed to take some shear load and in the case of tension the rivets takes some axial load, as explained in section 3.1.5.

To compensate for the contact between the V-stay anchorage and the cross-member plate in compression a back-support consisting of a number of bar-elements is used to simulate this contact. This keeps the two parts apart

and leads to a more realistic result. Thus, the back-support is only present in the model with the compressive load and not in the model with tensile load.

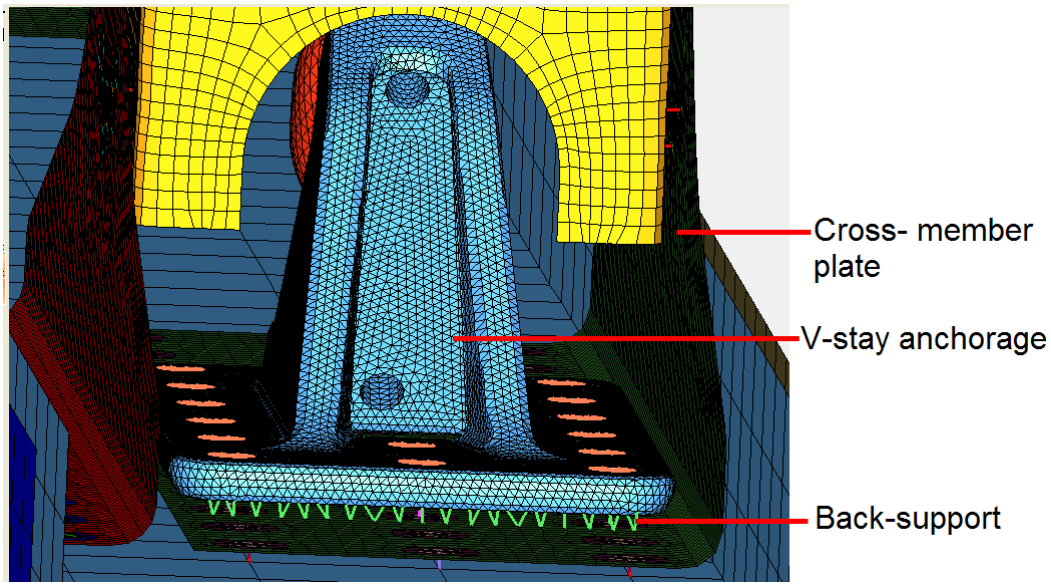

Figure 3.3: Model for compressive load with backsupport simulating contact

3.1.7 Fatigue life calculations

For the constant amplitude testing the fatigue life is simply estimated using an S–N curve, adopting peak local stresses. This will give a suitable load level to start the tests at, but since there are large uncertainties in this use of S–N curves the load level probably needs to be adjusted along the way.

The fatigue life calculations for the spectrum load are performed in LMS Falancs. The program employs stresses from the Nastran solver to estimate the damage in all selected parts of the FE model. The fatigue calculations only consider the surface elements of the V-stay anchorage. The dynamic load signal has been recorded by strain gauges mounted to the V-stay of a truck running at Volvo's testing ground. Some parts of the recorded signal do not inflict any significant damage to the studied component and are therefore excluded from the calculations. The composition of the spectrum load, as seen in figure 3.4, is typical for what an operational V-stay anchorage is subjected to during its service life. The signal is however scaled so that the maximum load is 100 kN. This means that the material damage of the component presented in this thesis can not be used to draw any conclusions about the actual fatigue life of a V-stay anchorage of an operational truck. The damage calculations are solely used to compare different FE models and to find a suitable maximum load for the fatigue testing. Material data for 500-7 are used in the fatigue evaluations. The S–N curve is extrapolated below the fatigue limit, as indicated in figure 2.2. The stress response from the 100 kN load in the FE analysis is used to calculate the stress response for the forces in the dynamic signal.

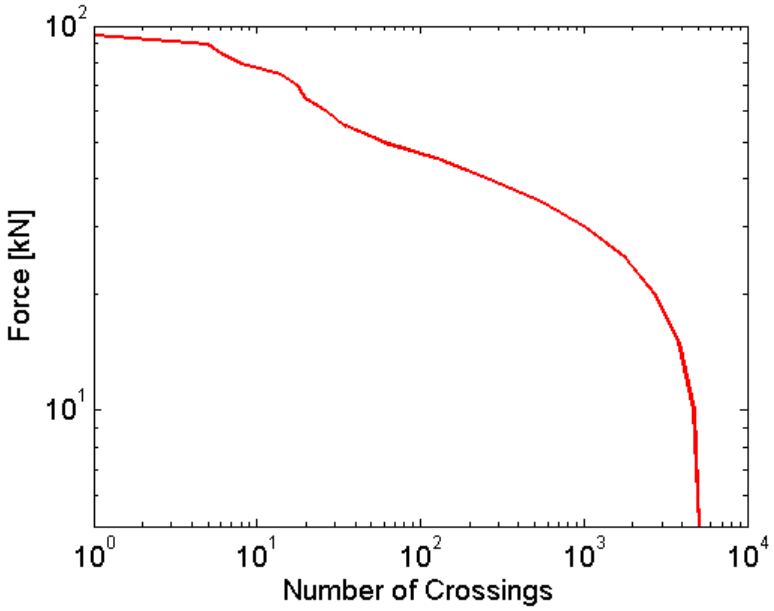

Figure 3.4: Load spectrum – level crossing

In the LMS Falancs calculations, the same FE model is used both for compressive and tensile loading. This is because it is not possible to differentiate between compression and tension in Falancs since the FE models are not identical, (due to the bars simulating contact and the extra rivet elements sustaining axial forces in compression, see 3.1.5). For comparison, a method using Matlab is used to perform this differentiation. The part of the load signal corresponding to compression will employ stresses from the compressive model and the part corresponding to tension will employ stresses from the tensile model. This means that the stress response will be linear for both compressive and tensile loads, but that the inclination will differ between them. This is indicated in figure 3.5, which explains how the stress response in a point is calculated in the Matlab model for the applied forces. The damage is calculated in a number of hotspots where the component experiences the highest stress levels. In this way the damage will be calculated in the same way as in Falancs but with the possibility to differentiate between tension and compression.

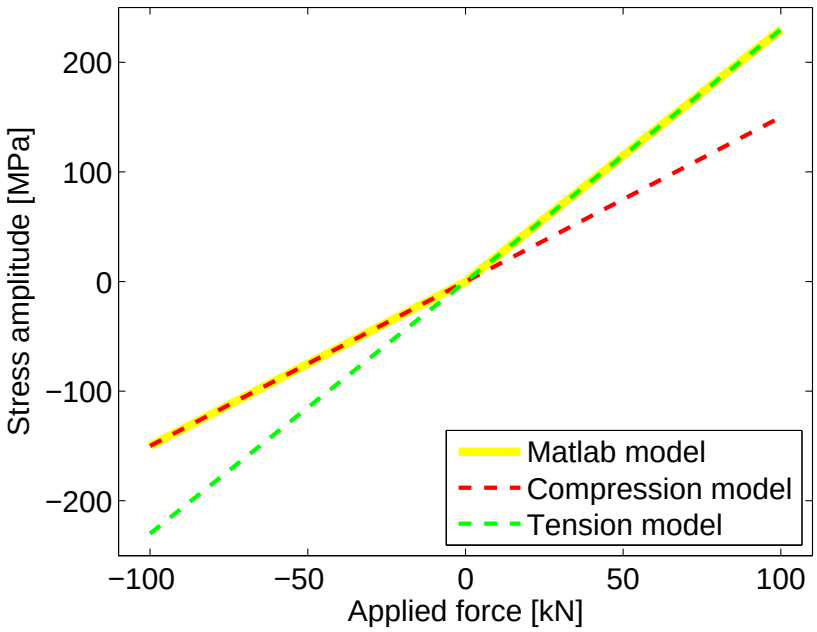

Figure 3.5: Comparison of stress response in a single point for linear models for compression and tension used in Falancs and the combined method used in Matlab

3.2 Fatigue testing

The hydraulic cylinder used in the rig has a maximum capacity of 25 tonnes ($\backsim$250 kN). The load signal used is sinusoidal. Two components are mounted, one at each end of the hydraulic cylinder. The two components are tested at the same time. They will be equally loaded by the hydraulic cylinder. Since the rig is vertically mounted, the lower anchorage will also carry the weight of the hydraulic cylinder. However, the weight will only correspond to roughly 1 % of the applied load and is therefore not assumed to affect the fatigue live significantly. A picture of the physical test rig can be seen in figure B.5 in appendix B.

4 Results and discussion

When comparing simulations the von Mises stress is used since this is a general representation of a multiaxial state of stress. Since the component is loaded with a single load in a linear model, the principal stresses will not rotate and calculations have shown that the stress field near the stress concentrations is close to uni-axial. In the fatigue life estimations, the largest principal stress is considered, since this is an important measure of the stress state, from a fatigue point of view. In the report only stress levels from a number of hot-spots are presented. These are sites, presented in figure 4.1, experiencing the highest stress levels in the FE analysis and therefore most likely to experience fatigue damage. The sites around the rivets and bolts experience singularities arisen from the use of rigid stars in the modeling of the fasteners. This rigidity causes very high and unphysical stresses which are disregarded. The complete stress contours in the V-stay anchorage for all different cases are presented in Appendix A.

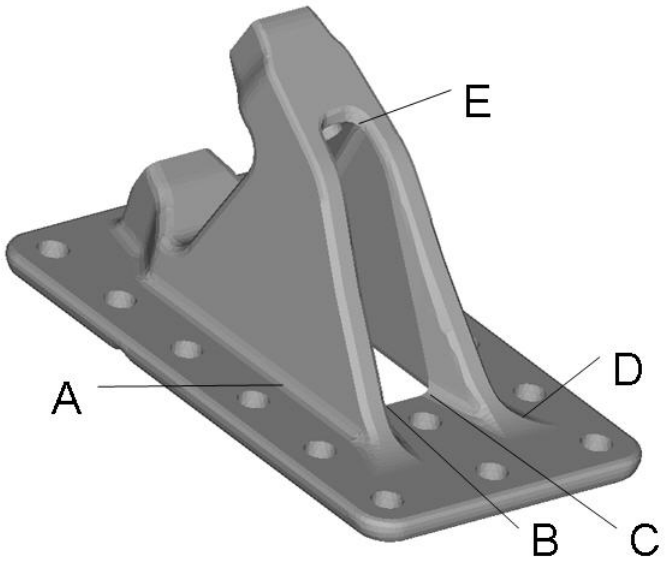

Figure 4.1: Hotspots where stress levels are presented

4.1 Rig design

The influence from a number of parameters was examined in the FE analyses. In table 4.1 the von Mises stress in the final rig model compared to the truck-like reference can be seen. The stresses are very near the goal of staying within a 10 % difference between the two cases.

Table 4.1: Comparison of von Mises stress magnitudes for the truck-like model and the final rig

Pos	Truck-like model [MPa]	Final rig [MPa]	Difference
A	178	188	5,62%
B	177	177	0,00%
C	185	189	2,16%
D	201	180	-10,45%
E	248	224	-9,68%

In the following results, the stress responses in the final rig model as presented above are used as a reference. The influence from each parameter is examined separately, meaning that the models are identical except from the examined parameter, e.g. load angle, adjacent components, fastener modeling etc. The exception is the rig length examination, where the stress response is compared to the truck-like model.

4.1.1 Load angle

Two different load angles were examined through numerical simulations. One corresponding to the correct load angle, 28.2°, in a truck. The other corresponding to a load angle of 23° which is achieved if an unmodified cross-member is used. This is described more extensively in section 3.1.3.

Table 4.2: Comparison of von Mises stress for two different load angles

Pos	Load angle 28.2° [MPa]	Load angle 23° [MPa]	Difference
A	188	196	4,26%
B	177	181	2,26%
C	189	196	3,70%
D	180	198	10,00%
E	223	259	16,14%

The large difference between the two cases suggests that the load angle needs to be kept as in an operational truck. To achieve this the frame need to be wider. This is done by welding an extra piece, 130 mm in length, in the middle of the two cross-members making the frame 980 mm wide. This will secure the correct load angle for all tested components, $\arcsin(755/1600) = 28.2°$, see figure 4.2.

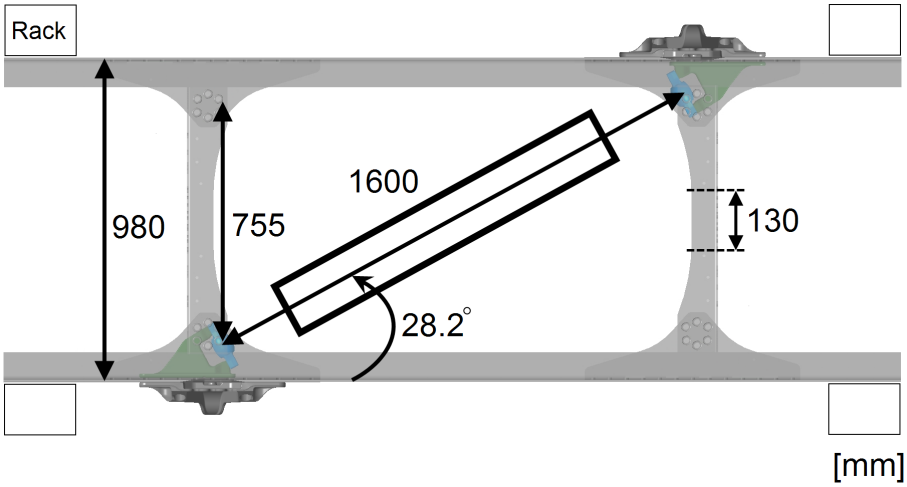

Figure 4.2: Sketch of modified rig

4.1.2 Rig length

In table 4.3, the stress response in the 4 m rig is compared to the truck-like model. The frame of the rig is lengthened so that the distances between the V-stay anchorages and the racks are longer than in the 3 m model. The distance between the two cross-members is kept constant between the two models.

Table 4.3: Comparison of von Mises stress for a truck-like model and a 4m rig

Pos	Truck-like model [MPa]	Rig – 4 m [MPa]	Difference
A	178	187	5.06%
B	177	177	0.00%
C	185	189	2.16%
D	201	184	-8.46%
E	248	228	-8.06%

As seen in table 4.3 the stress response in the 4m rig is closer to the truck-like model than what the final 3 m rig provides. The vertical mounting wall is however only 3m, whereas a longer rig would require more space. Further, the deformation magnitudes would increase. The benefits in stress distribution for the longer rig are therefore not considered to weigh out the drawbacks.

4.1.3 Adjacent components

On the outside of the frame of the truck there is a reaction rod bracket mounted, see figure 1.3, providing some stiffness to the area. It is assumed to affect the stress response in the V-stay anchorage and the influence is therefore examined through numerical simulations. A FE analysis of the rig with and without the reaction rod bracket is performed and the stress response is presented in table 4.4.

Table 4.4: Comparison of von Mises stress with and without reaction rod bracket, (RRB)

Pos	with RRB [MPa]	without RRB [MPa]	Difference
A	188	128	-31,91%
B	177	258	-10,73%
C	189	179	-5,29%
D	180	213	18,33%
E	223	270	21,08%

As seen in table 4.4 the reaction rod bracket has a significant effect on the stress field. This leads to the conclusion that it needs to be included in the physical test rig and in the FE model to get a reasonable stress responses.

4.1.4 Modal analysis

The lowest eigenfrequency, calculated in the modal analysis, of the rig is 59.6 Hz. The frequency is well above the expected test frequency of about one Hertz. This means that there should be no problem with resonance in the rig.

4.2 FE-model

4.2.1 Modeling fasteners

The fasteners have been modeled in two different ways as described in 3.1.5. In the idealized case the rivets can only sustain shear loads and the bolts only axial loads. In the second, more realistic, case the fasteners are modeled so that the rivets are allowed to also take some load axially and the bolts are allowed to take some shear loading. The layout of the fasteners can be seen in figure 4.3.

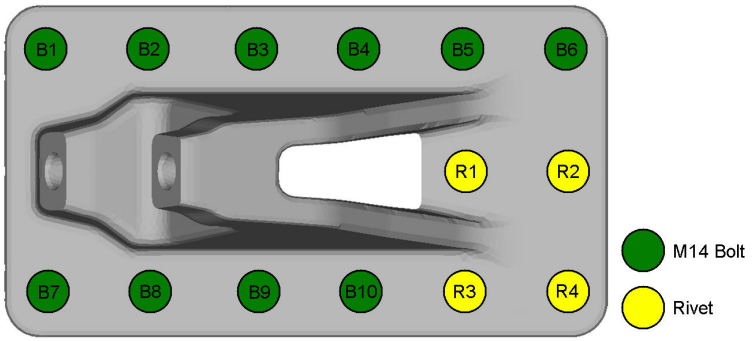

Figure 4.3: Positions of fasteners

The shear and the axial forces sustained by the fasteners in the idealized and the more realistic case are presented in table 4.5. The sustained forces in the more realistic case are at levels judged to be reasonable, as discussed in section 3.1.5. Suitable diameters have been found iteratively. The bolts are modeled with an extra rod with 2.2 mm radius and a length of 17 mm. The length of the extra rods is just a consequence of how the components

are modeled. Three of the rivets, R1-R3, are modeled with 1mm radius and rivet R4 with 0.74 mm radius. All extra rivet bars are 4 mm in length.

Table 4.5: Loads in rivets and bolts

	Idealized fasteners		Realistic fasteners	
Fastener	Axial [kN]	Shear [kN]	Axial [kN]	Shear [kN]
B1	-2.44	0	-2.78	4.96
B2	-0.37	0	0.82	5.37
B3	0.97	0	2.12	5.11
B4	4.05	0	4.79	5.48
B5	7.64	0	7.81	6.30
B6	13.97	0	8.43	5.73
B7	-2.66	0	-3.28	4.47
B8	-1.27	0	0.11	4.43
B9	-1.07	0	1.44	4.80
B10	28.43	0	16.77	4.36
R1	0	52.08	2.18	17.95
R2	0	36.62	3.07	18.2
R3	0	14.84	3.04	14.57
R4	0	10.55	2.74	7.44

The sustained shear forces in the rivets are at a high level in the idealized case, especially for a dynamic load where fatigue must be considered. In the more realistic case the shear forces are sustained by all fasteners in the model but to a higher degree by the rivets.

The stress response in the V-stay anchorage is severely influenced by the fastener modeling. The stresses in the hotspots are significantly higher in the idealized case, as seen in table 4.6. The displacement in the riveted corner of the anchorage is judged to be larger than realistic. This is probably due to the large distance to a bolt in that corner; since the rivets are idealized the corner is free to deflect axially. The anchorage will bend approximately along a line passing through bolt 6 and 10, giving rise to high stresses in the vicinity.

Table 4.6: Comparison of von Mises stress for idealized and realistic fasteners

Pos	Realistic [MPa]	Idealized [MPa]	Difference
A	188	310	64.89%
B	177	428	141.81%
C	189	269	42.33%
D	180	285	58.33%
E	223	351	57.40%

4.2.2 Load case

Since the solver is linear, changing from tension to compression in the model would only change sign of the principal stresses. Here the model for compression has been modified with a back-support to simulate contact between the cross-member and the V-stay anchorage. This influences the stress response, presented in table 4.7, significantly since the deformation shape is altered. In

addition to the back-support, rivets are modified not to take any axial force but this is not assumed to affect the stress response as much.

Table 4.7: Comparison of von Mises stress for compression and tensional load prescribed by a model including back-support

Pos	Tension [MPa]	Compression [MPa]	Difference
A	188	146	-22.34%
B	177	55	-68.93%
C	189	159	-15.87%
D	180	184	2.22%
E	223	183	-18.30%

The large difference between compression and tension, as seen in table 4.7, suggest that a linear model is not the best way to model the component.

4.2.3 Final rig model

A sketch of the final rig, based on the results above, is presented in figure 4.4. The load angle is the same as in an operational truck, the reaction rod bracket is mounted outside the frame and the total length is 3 m.

The FE model, assumed to give the most realistic stress response is when the fasteners are modeled with the alternative model, described in section 3.1.5 and when there is a differentiation between tension and compression.

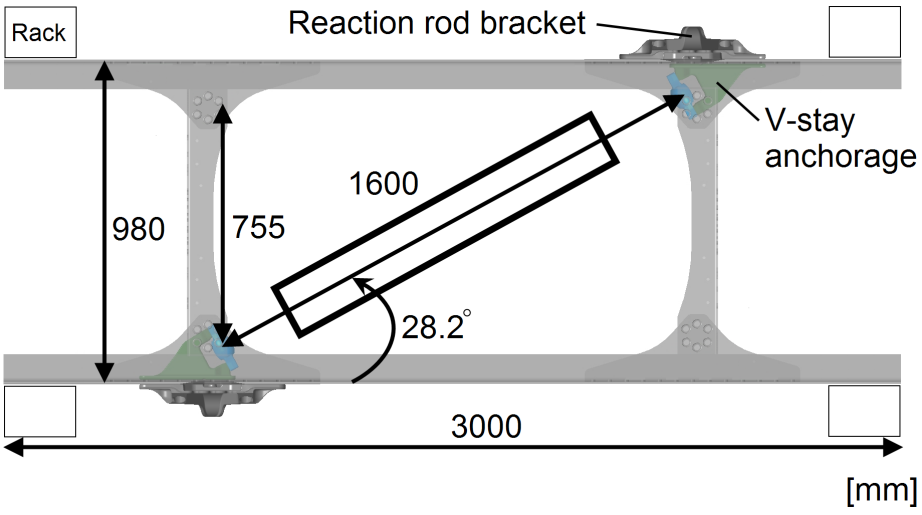

Figure 4.4: Sketch of final rig

4.3 Fatigue life estimations

Even though the stress response does not differ more than roughly 10 % between the final rig and the truck-like model, the difference in material damage is far larger. This is due to the logarithmic nature of fatigue strength. The material damage in the hotspots are presented in table 4.8. To see the severe influence from higher stress levels, the fatigue damage in the model with idealized fasteners is also evaluated and presented in table 4.9. The

estimated fatigue damage presented corresponds to the damage after one operational life-time with a maximum load of 100 kN. An estimated fatigue damage of 100 % would correspond to failure. Contour plots of the material damage for the three models can be found in appendix A.

Table 4.8: Estimated fatigue damage in Falancs

Pos	Truck-like reference	Rig – Tension	Difference
A	1.27%	1.66%	30.16%
B	0.69%	0.71%	1.88%
C	0.95%	1.06%	11.66%
D	1.60%	0.91%	-43.26%
E	3.33%	2.01%	-39.53%

Table 4.9: Estimated fatigue damage in Falancs

Pos	Realistic	Idealized	Difference
A	1.66%	17.80%	974.11%
B	0.71%	46.36%	6466.01%
C	1.06%	4.92%	362.37%
D	0.91%	7.46%	724.53%
E	2.01%	17.14%	751.42%

The evaluated stresses are pre-processed using Falancs and pertinent material damages in the hotspots are presented in table 4.10. The stress responses from the compression and the tension models are also combined into a material damage computation performed in Matlab presented in the same table.

Table 4.10: Estimated fatigue damage from ”tension” and ”compression” models and a combination of these models

Pos	Tension	Compression	Combination
A	1.66%	0.53%	1.06%
B	0.71%	0.00%	0.15%
C	1.06%	0.48%	0.77%
D	0.91%	1.23%	1.03%
E	2.01%	0.89%	1.38%

As seen in table 4.10 the maximum damage using the Matlab method for a spectrum load with a maximum load of 100 kN is 1.38 %. This means that the component would survive $100/1.38 = 72.5$ lifetimes, with a 50 % failing rate at this load level. The time to perform this test would be inconveniently long, even if the signal is significantly shortened, which means that the maximum load of the signal must be magnified to obtain reasonable testing times. The material in the V-stay anchorages must however be kept from stresses above the yield limit.

4.4 Material investigation

One V-stay anchorage cast in 500-7 and one in 500-14 was sent to Volvo Materials technology for examination. Four specimens cut from sections with different thicknesses were used in the investigations. The hardness was measured at three points in each of the four specimens. The averaged material properties all fulfill the required demands in the proposed EN standard, [15]. However, one of the specimen made from 500-14 had a nodularity as low as 74 %, but since this specimen was cut from a low stressed area it is assumed not to affect the fatigue life. As seen in table 4.11 the hardness variation is very low for 500-14, as expected for this material. The microstructure in 500-14 is allowed to contain up to 5 % pearlite according to [15], but the tested specimens contained none. All V-stay anchorages used in the fatigue tests are from the same batches as the investigated ones. The chemical compositions have also been analyzed by Volvo Materials technology and are presented in table 4.12. The values in table 4.11 and 4.12 are as expected. The main differences are that the 500-10 material has a lower carbon content, higher silicon content and a lower cupper content. Additional information about the material examination can be found in appendix C.

Table 4.11: Material properties of a V-stay anchorage in 500-14

Material	Nodularity [%]	Nodule count [/mm^2]	Max flake graphite rim depth [mm]	Amount pearlite [%]	Hardness [HBW]
500-14	82	180	0.2	0	192±5
500-7	91	270	0.25	40	197±9

Table 4.12: Chemical composition of a V-stay anchorage [wt%]

Material	C	Si	Mn	P	S	Cr
500-14	3.01	3.62	0.26	0.008	0.011	0.03
500-7	3.65	2.39	0.25	0.008	0.008	0.05

Ni	Mo	Cu	Sn	Ti	V	Mg
0.01	<0.01	0.006	0.006	0.011	<0.005	0.045
0.02	<0.01	0.30	0.005	0.005	0.010	0.044

4.5 Fatigue tests

4.5.1 Proposed test scheme

Since there is expected to be a large scatter in fatigue life between components, a fairly large number of samples would be required to draw conclusions about the material's absolute fatigue strength and its statistical distribution. It is, for many reasons, not possible to test such a large number of components in both materials. An estimation is that five samples of each material at each stress amplitude is sufficient to capture any significant difference in fatigue strength between the two materials. A few samples tested with spectrum load would be interesting in order to be able to compare with the

results from constant amplitude tests. Since a finite life is sought there is however a risk that the peak loads of the dynamic signal will cause yielding of the material. The peak load level in table 4.13 should for this reason not be taken as final. It is likely that it needs to be calibrated until a functional level is achieved.

Table 4.13: Proposed test scheme

Case	Material	Load type	Peak load [kN]	PCS
1	500-7	Constant	100	2
2	500-7	Constant	150	5
3	500-14	Constant	150	5
5	500-7	Constant	175	5
6	500-14	Constant	175	5
7	500-7	Spectrum	160	3
8	500-14	Spectrum	160	3
9	500-7	Spectrum	190	3
10	500-14	Spectrum	190	3

4.5.2 Fatigue tests

In figure 4.5 the number of cycles to failure for five tests of 500-7 V-stay anchorages are plotted against the stress amplitude in hotspot E from the FE simulations with a tensile load. An S–N curve for 50 % failure rate for the 500-7 material from [14] is plotted as reference. It should be noted that the V-stay anchorages are shot-peened after the casting to clean them from moulding sand. This introduces compressive stresses at the surface of the component which can be beneficial from a fatigue point of view.

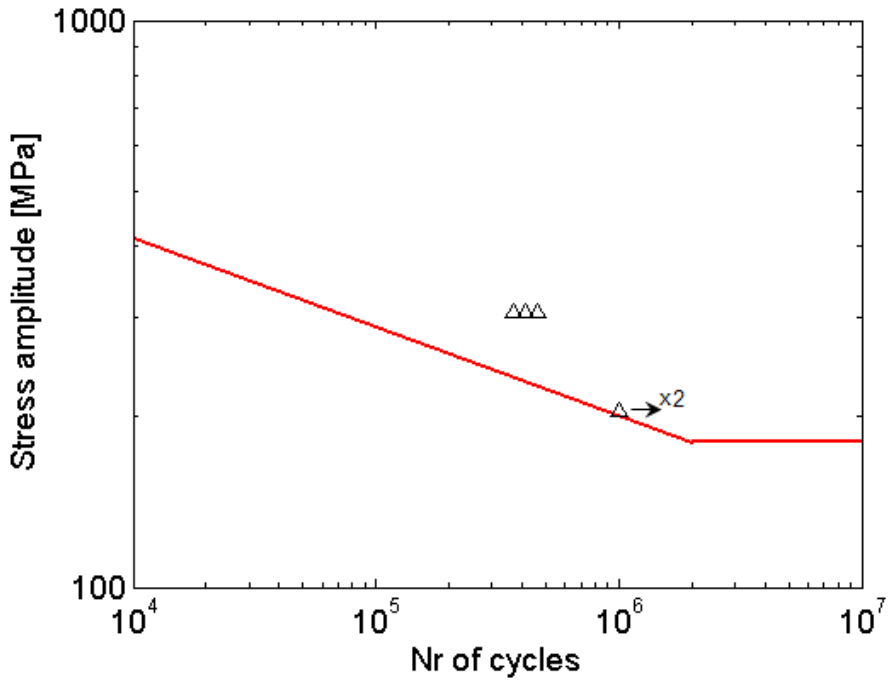

Figure 4.5: Results from fatigue testing of V-stay anchorage in 500-7 material

One of the tested V-stay anchorages that failed due to fatigue has been examined by Volvo Materials technology. There are two fatigue crack initiation sites in the examined V-stay anchorage. When the first crack is formed, the other site is subjected to higher stress leading to a second fatigue crack. The fatigue crack initiation sites leading to failure, see figure 4.6, are situated close to hotspot E as expected. All tested V-stay anchorage that has failed due to fatigue has similar failure modes.

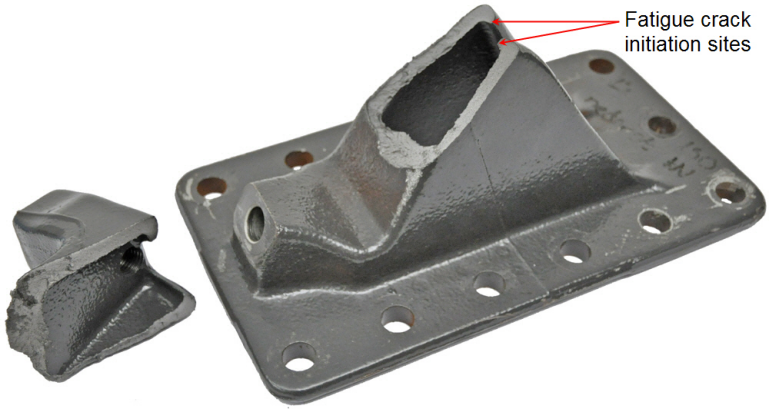

Figure 4.6: Fatigue tested V-stay anchorage in 500-7

5 Conclusions

Theoretically evaluated stress magnitudes in a V-stay anchorage will together with experimentally found lives be used to construct an S–N curve. It is therefore important that the stress levels from the FE analyses are reliable. As shown in this thesis the predicted stress level is influenced by a number of parameters, such as the modeling of the fasteners and the contact between components. To get a clearer picture of the stress in the component, a contact analysis would be suitable. It would also provide the possibility to evaluate the validity of the linear approximation. This would be beneficial since a linear analysis requires a lot less modeling and solving time than a contact analysis. Here it should be noted that in conventional software for material damage calculations the stress is linearly scaled for all load levels. This means that a contact analysis would not be suitable for fatigue life calculations using conventional software.

Since the stresses are high in a number of hotspots in the V-stay anchorage the risk is that cracks initiate and propagate at different hotspots in different specimens. It would for this reason be beneficial if the tested component had only one hotspot with a significantly higher stress. This would ensure that all specimens crack in the same location and that the failure mode would be similar. Since the V-stay anchorage needs to be riveted, and that requires a special riveting machine, the down-time between failure and restart is quite long. If the tested component had only been fastened with bolts this time could be considerably shorter. To induce significant fatigue damage in the component the force amplitude needs to be fairly high, around 150 kN. This force amplitude will cause high stress levels also in other parts of the rig that may cause fatigue failure of supporting parts. A weaker test component would be practical since the demands on fatigue strength in other components of the rig would be lower.

The results show the importance of performing thorough preparations before fatigue testing if useful results are to be obtained. Calculations have shown that stress magnitudes easily differ 50 % between different models of the same component. This has a severe effect on the predicted fatigue life. Thus, FE simulations must be made reliable, taking all affecting parameters into account. It also means that physical fatigue testing must achieve the same conditions in the rig as in a real truck, if the component is to be evaluated in an absolute sense. If the test is used just to compare two materials or two designs this is less important.

The results from the manufacturer do not point towards any significant increase in fatigue strength in 500-14 as compared to 500-7. If the results from the testing planned in this thesis points in the same direction, further investigations of other solution strengthened SGI could be of interest. An interesting material here is EN-GJS-600-10 which contains even more silicon. 600-10 has a fatigue limit of 275 MPa in the proposed EN-standard, which is more than 20 % higher that of 500-7 and 500-14.

References

[1] A Björkblad. Fatigue assessment of cast components : Influence of cast defects. Doctoral thesis, Royal Institute of Technology, 2008.

[2] L E. Björkegren and K Hamberg. Silicon alloyed ductile iron with excellent ductility and machinability. *Proceedings of 2003 Keith Millis Symposium on Ductile Cast Iron*, 1:70–90, 2003.

[3] William D. Callister. *Materials science and engineering: an introduction*. Wiley, New York, N.Y, 2007.

[4] M. Dahlberg. Fatigue in nodular iron. Licenciate thesis, Department of Solid Mechanics, Royal Institute of Technology, 1997.

[5] Norman E. Dowling. *Mechanical behavior of materials: engineering methods for deformation, fracture and fatigue*. Pearson Prentice Hall, Upper Saddle River, N.J, 2007.

[6] C.M Ecob. A review of common metallurgical defects in ductile cast iron. http://www.elkem.no/dav/dfa48df95b.pdf.

[7] K. D. Millis et al. Cast ferrous alloy. us patent, 1949.

[8] M. Gagne and C. Labrecque. Ductile iron: Fifty years of continuous development. *Canadian Metallurical Quarterly*, 37:343–378, 1998.

[9] Espen Heier. Defect sensitivity in nodular cast iron under cyclic loads. Licentiate thesis, Engineering Metals, Chalmers University of Technology, 1998.

[10] Anders E. W. Jarfors. *Tillverkningsteknologi*. Studentlitteratur, Lund, 2006.

[11] Rikard Källbom. Chunky graphite in heavy section ductile iron castings. Licentiate thesis, Materials and Manufacturing Technology, Chalmers University of Technology, 2006.

[12] Dr. Richard Lärker. Solution strengthened ferritic ductile iron iso 1083/js/500-10 provides superior consistent properties in hydraulic rotators. *China Foundry*, 6:343–351, 2009.

[13] Marie Mörtsell. Crack initiation in nodular cast iron. Licentiate thesis, Materials and Manufacturing Technology, Chalmers University of Technology, 2005.

[14] J Nilsson. Dimensioneringsfilosofier och materialdata för segjärn. Svenska Gjuteriföreningen, 1997.

[15] prEN 1563:2009. Founding - speroidal graphite cast iron, 2009.

[16] J Salmi. Solution strengthened ferritic ductile iron: Foundary process, machinability and tool wear. Master's thesis, Tampere university of technology, 2010.

Appendix A

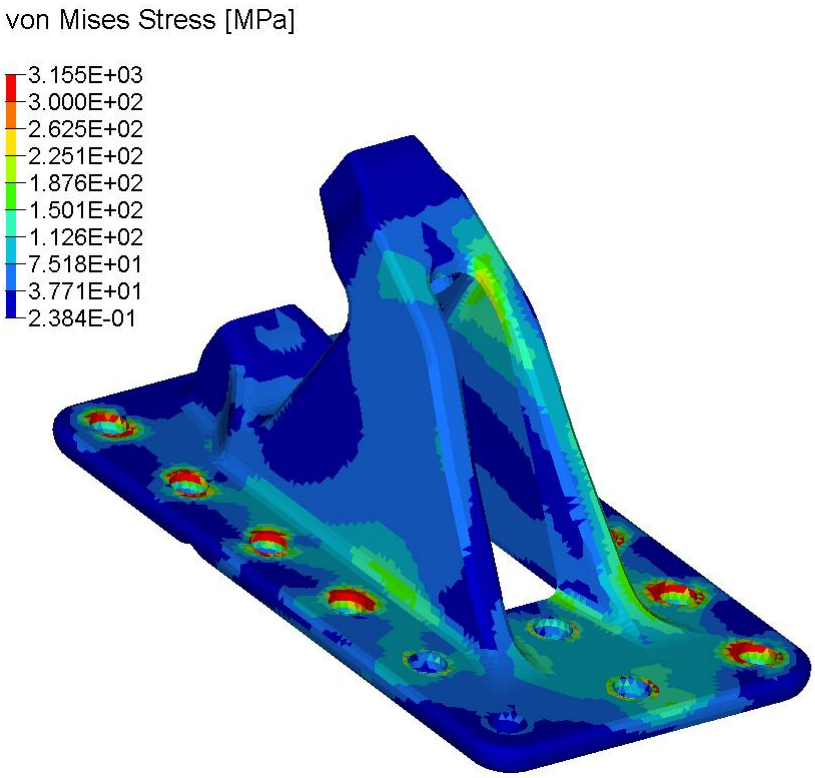

Hot Spots

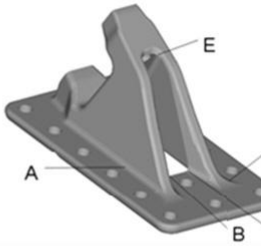

Position	vM stress [MPa]
A	178
B	177
C	185
D	201
E	248

Figure A.1: Stress response in truck-like model

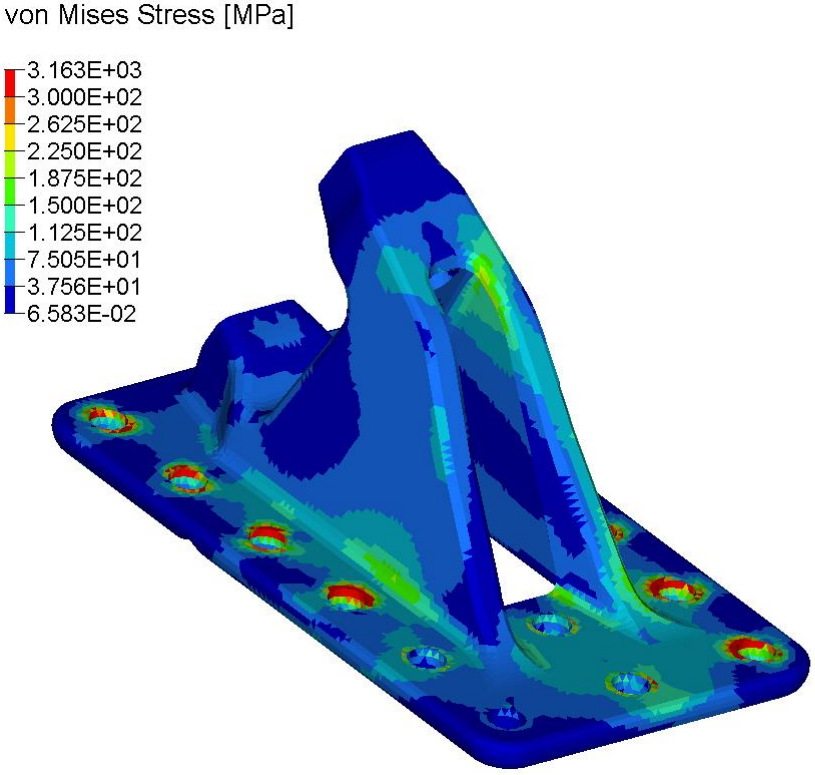

Hot Spots

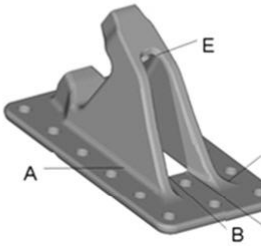

Position	vM stress [MPa]
A	188
B	177
C	189
D	180
E	224

Figure A.2: Stress response in final rig model

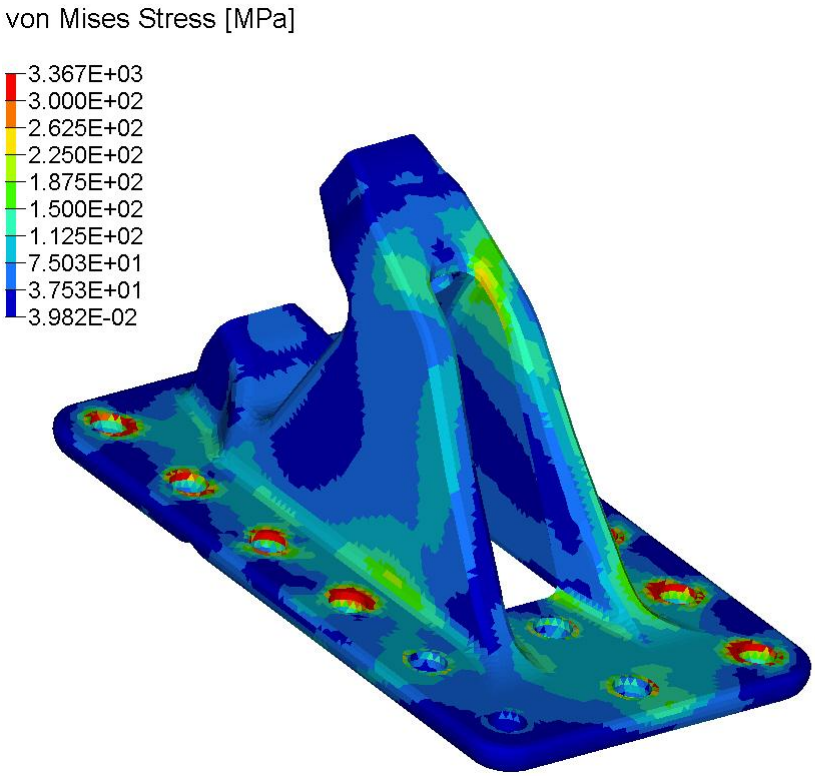

Hot Spots

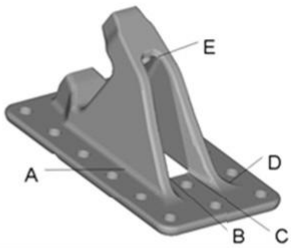

Position	vM stress [MPa]
A	196
B	181
C	196
D	198
E	259

Figure A.3: Stress response from 23° load angle

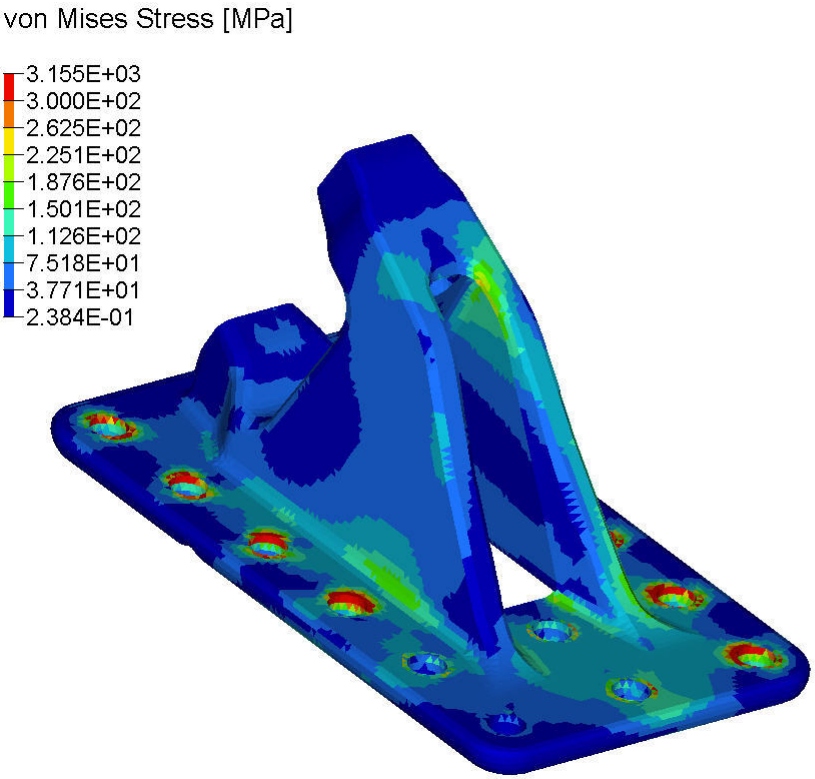

Hot Spots

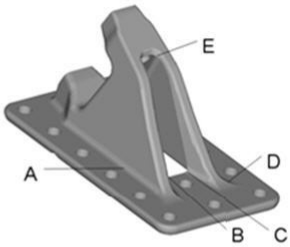

Position	vM stress [MPa]
A	187
B	177
C	189
D	184
E	228

Figure A.4: Stress response in 4m rig model

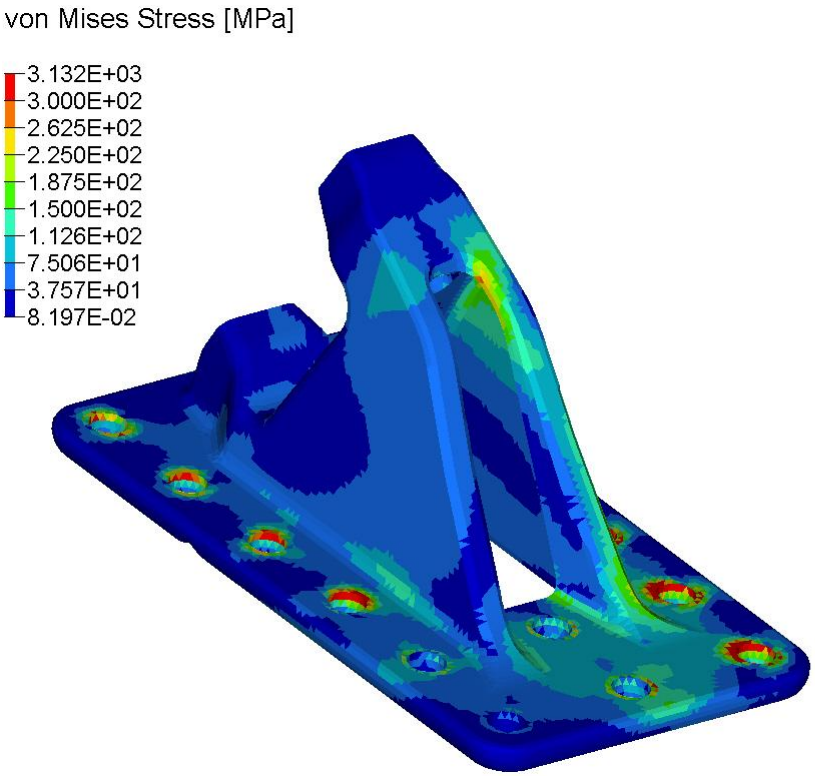

Hot Spots

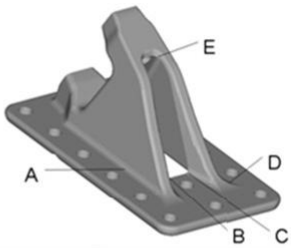

Position	vM stress [MPa]
A	128
B	158
C	179
D	213
E	270

Figure A.5: Stress response in model without reaction rod bracket

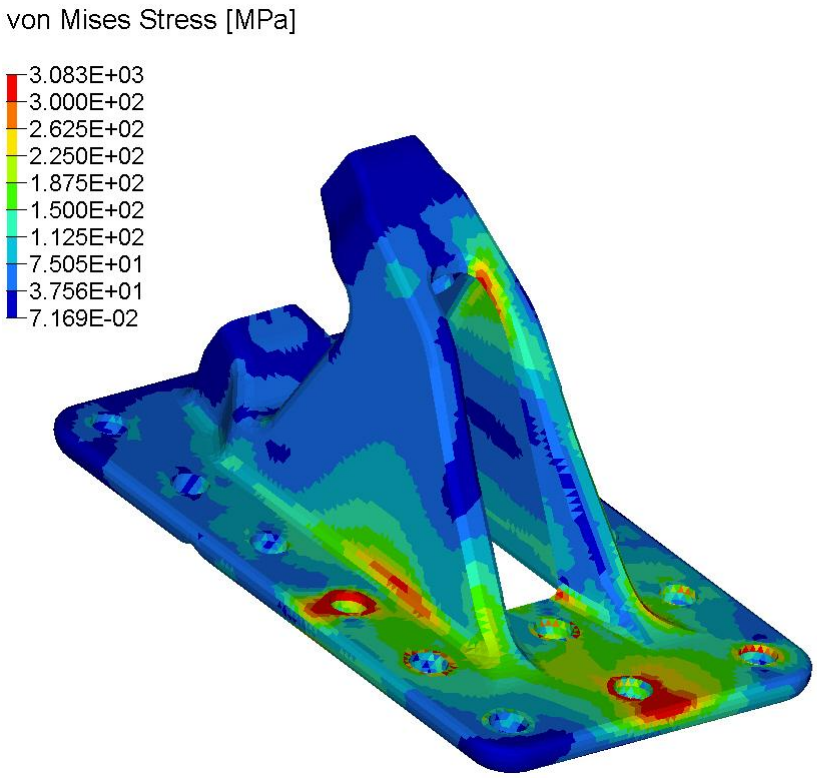

Hot Spots

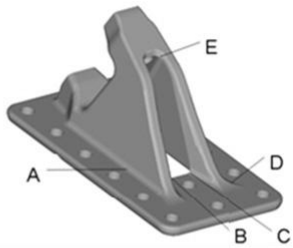

Position	vM stress [MPa]
A	310
B	428
C	269
D	285
E	351

Figure A.6: Stress response in model with idealized fasteners

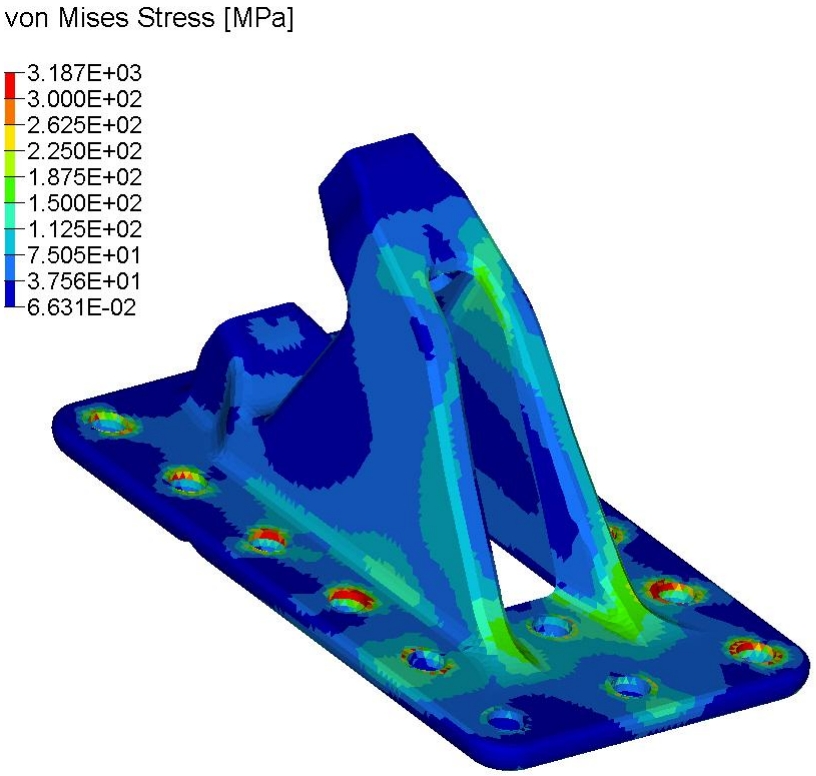

Hot Spots

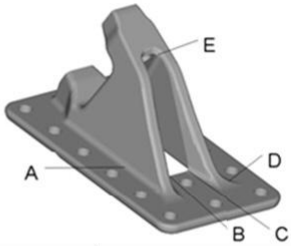

Position	vM stress [MPa]
A	146
B	56
C	159
D	184
E	183

Figure A.7: Stress response when loaded in compression

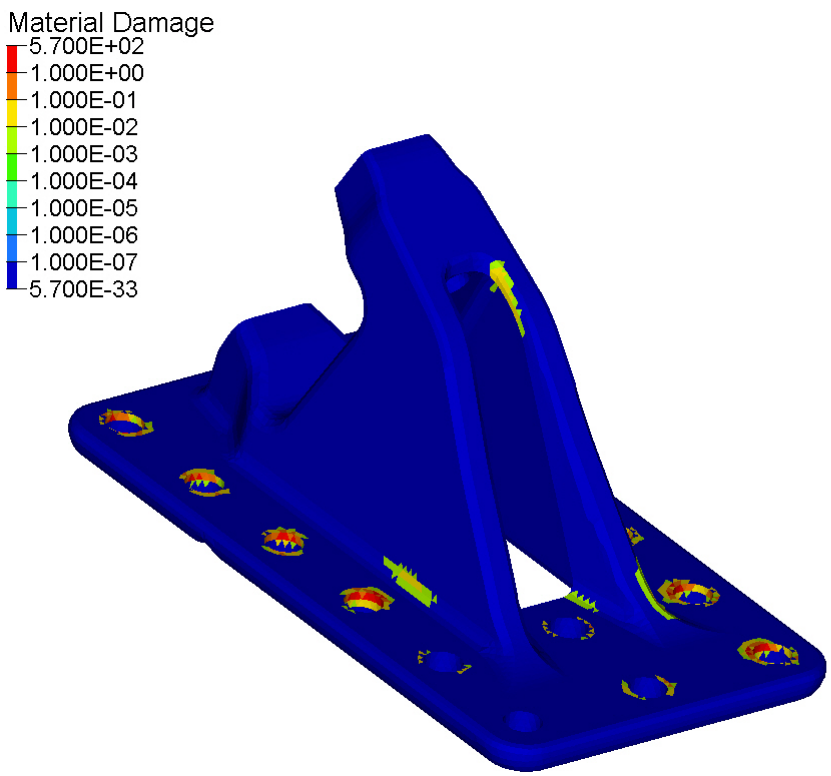

Hot Spots

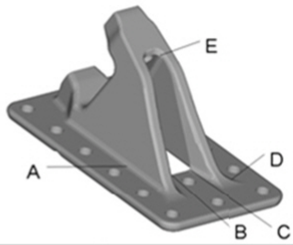

Position	Damage [%]
A	1,27%
B	0,69%
C	0,95%
D	1,60%
E	3,33%

Figure A.8: Estimated material damage in truck-like model

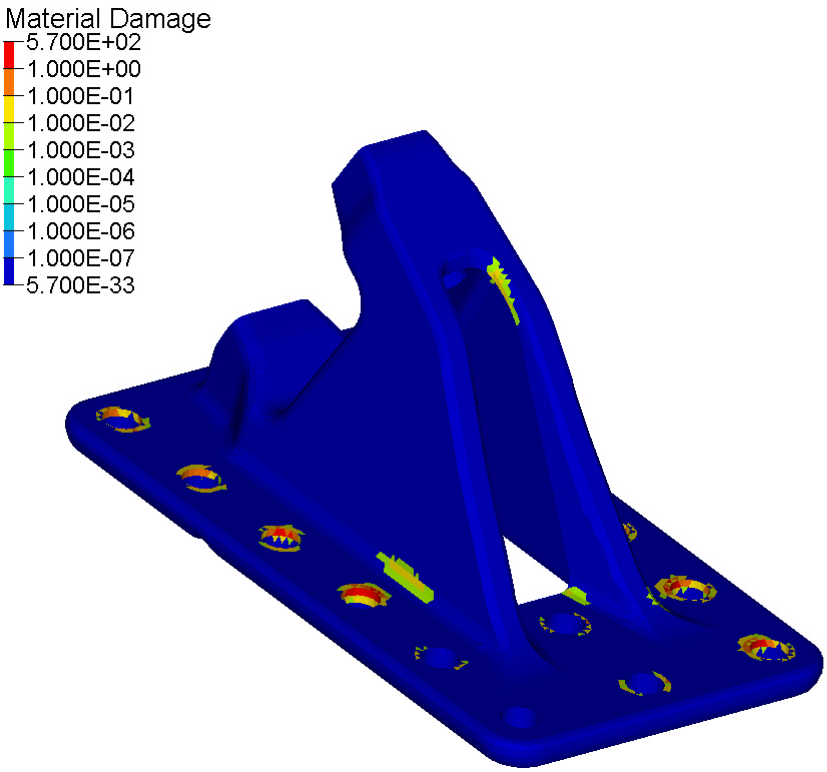

Hot Spots

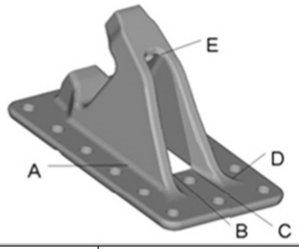

Position	Damage [%]
A	1,66%
B	0,71%
C	1,06%
D	0,91%
E	2,01%

Figure A.9: Estimated material damage in rig model

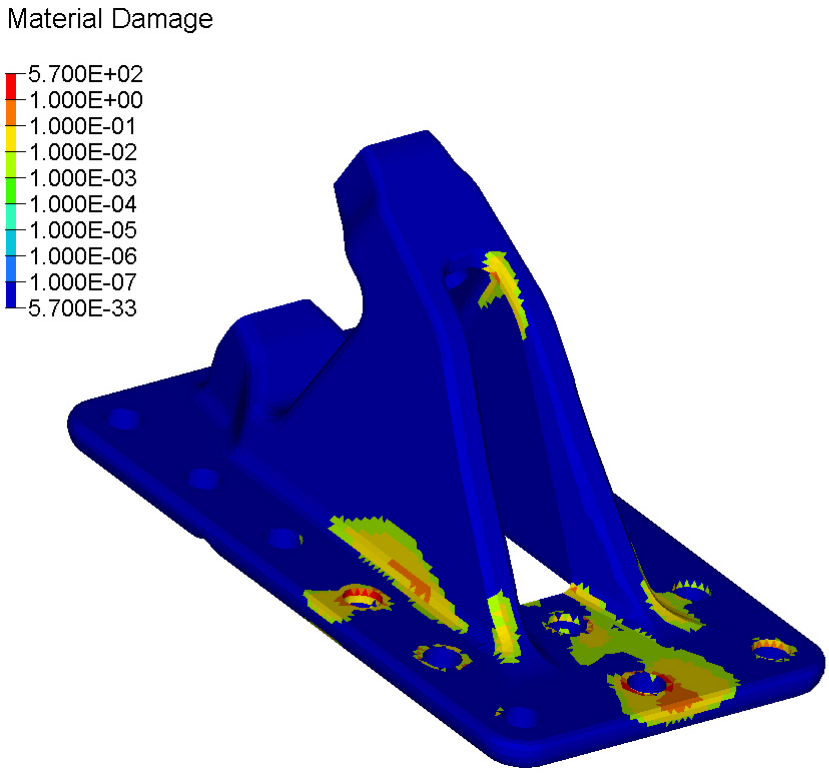

Hot Spots

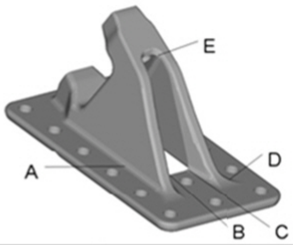

Position	Damage [%]
A	17,80%
B	46,36%
C	4,92%
D	7,46%
E	17,14%

Figure A.10: Estimated material damage with idealized fasteners

Appendix B

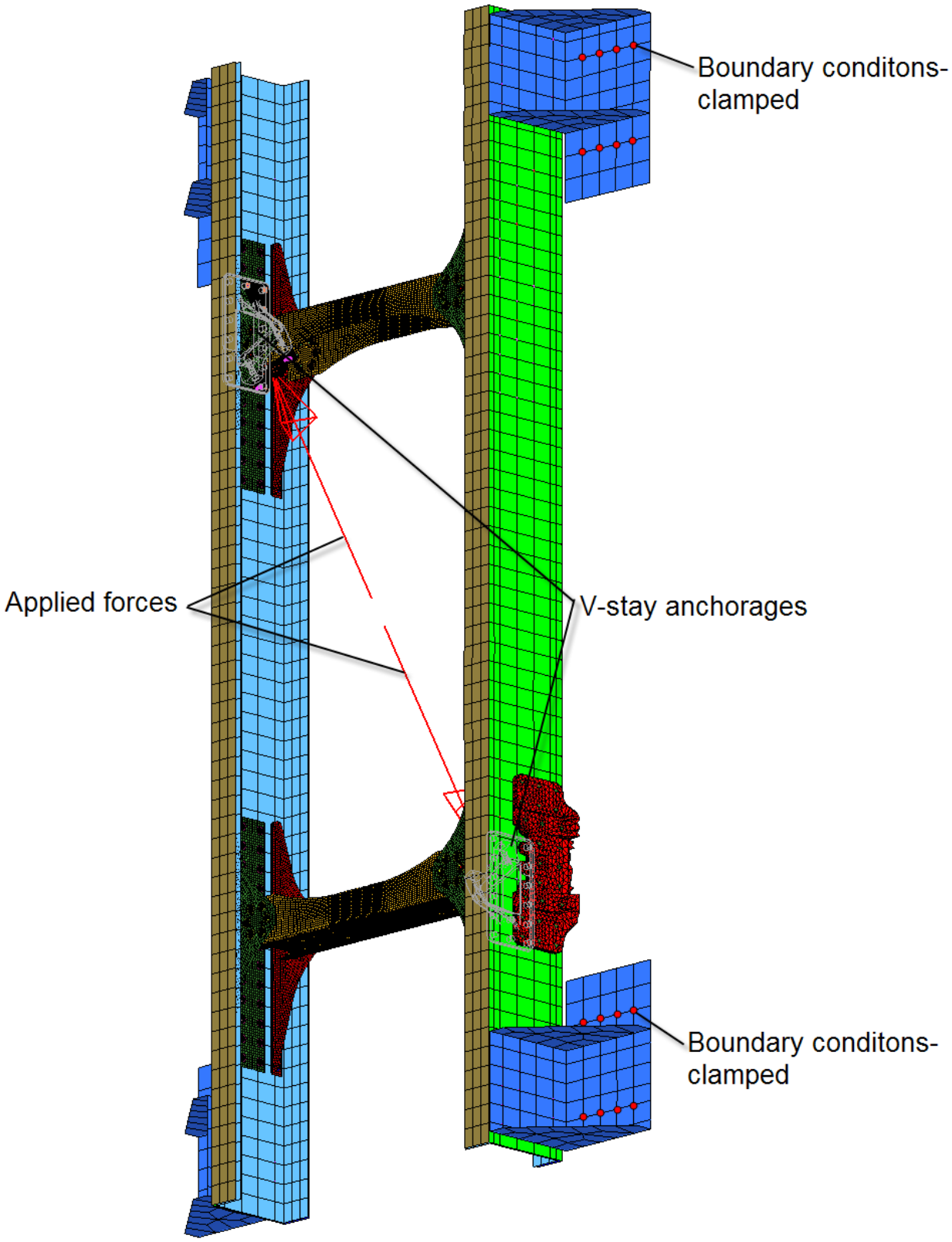

Figure B.1: Test rig model

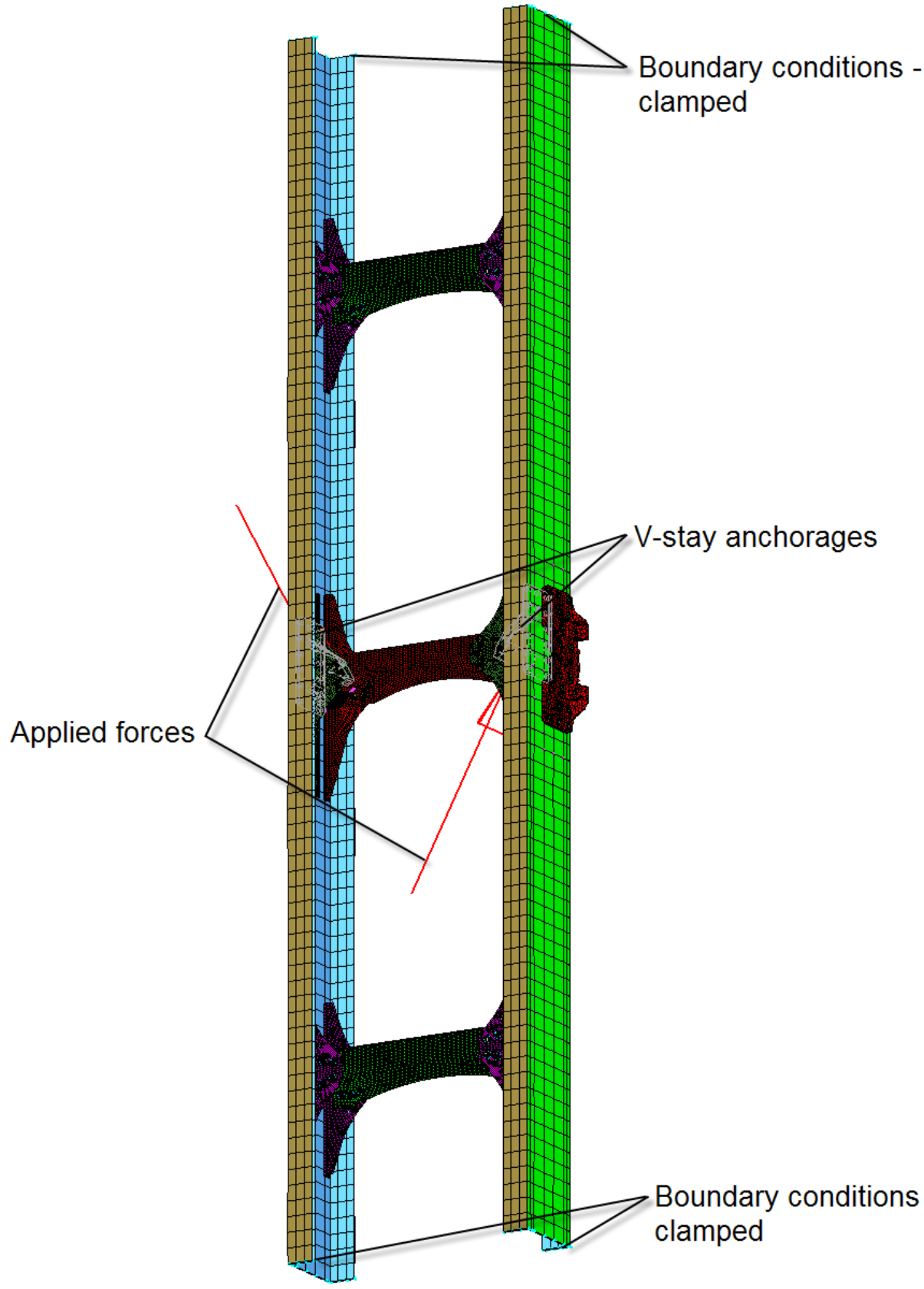

fro

Figure B.2: Truck-like model

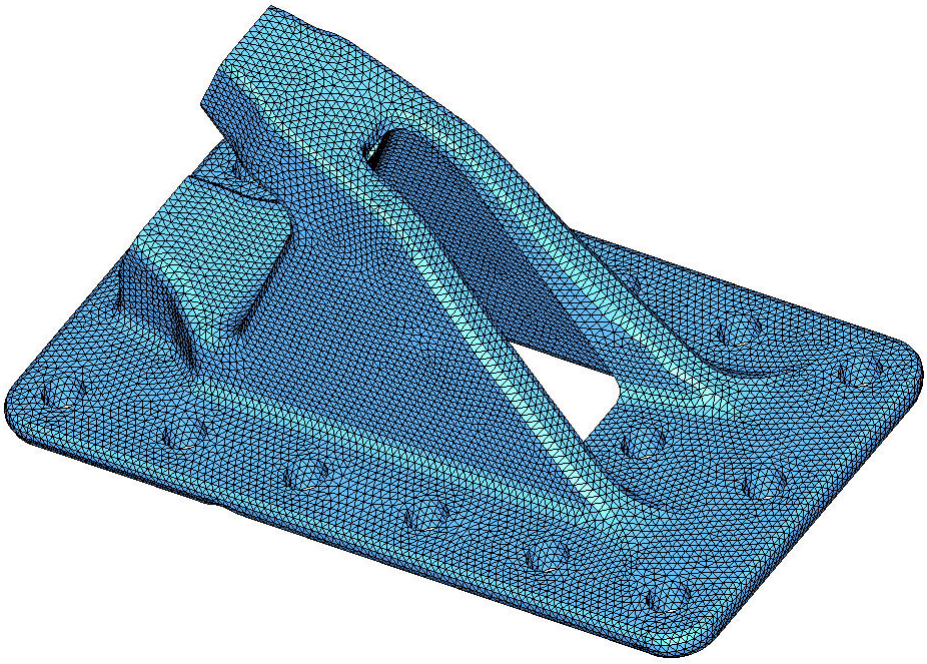

Figure B.3: V-stay anchorage mesh

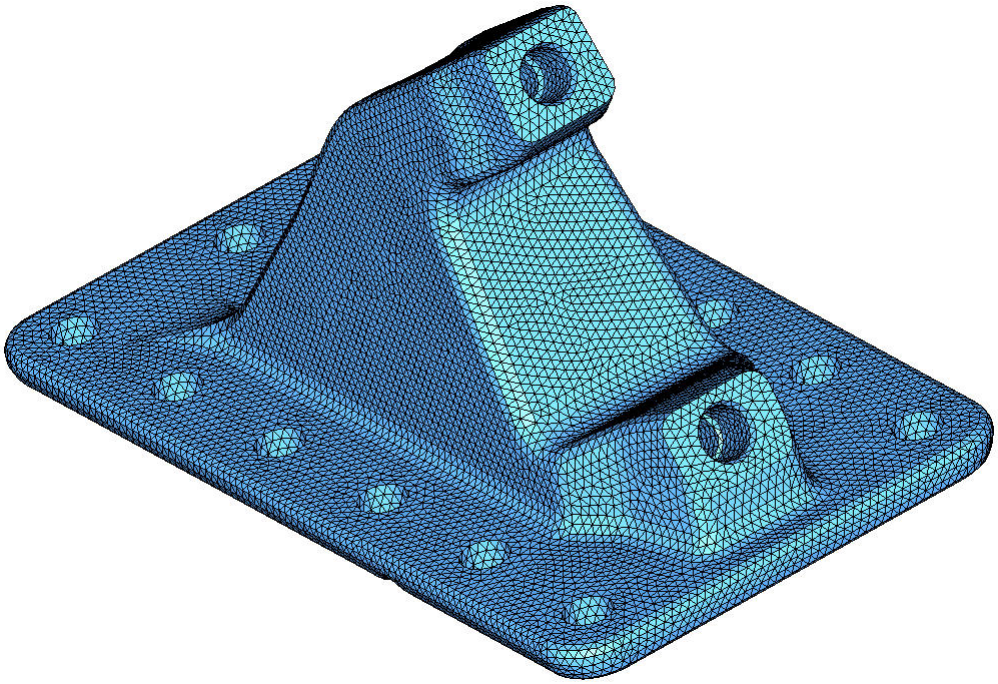

Figure B.4: V-stay anchorage mesh - opposite view

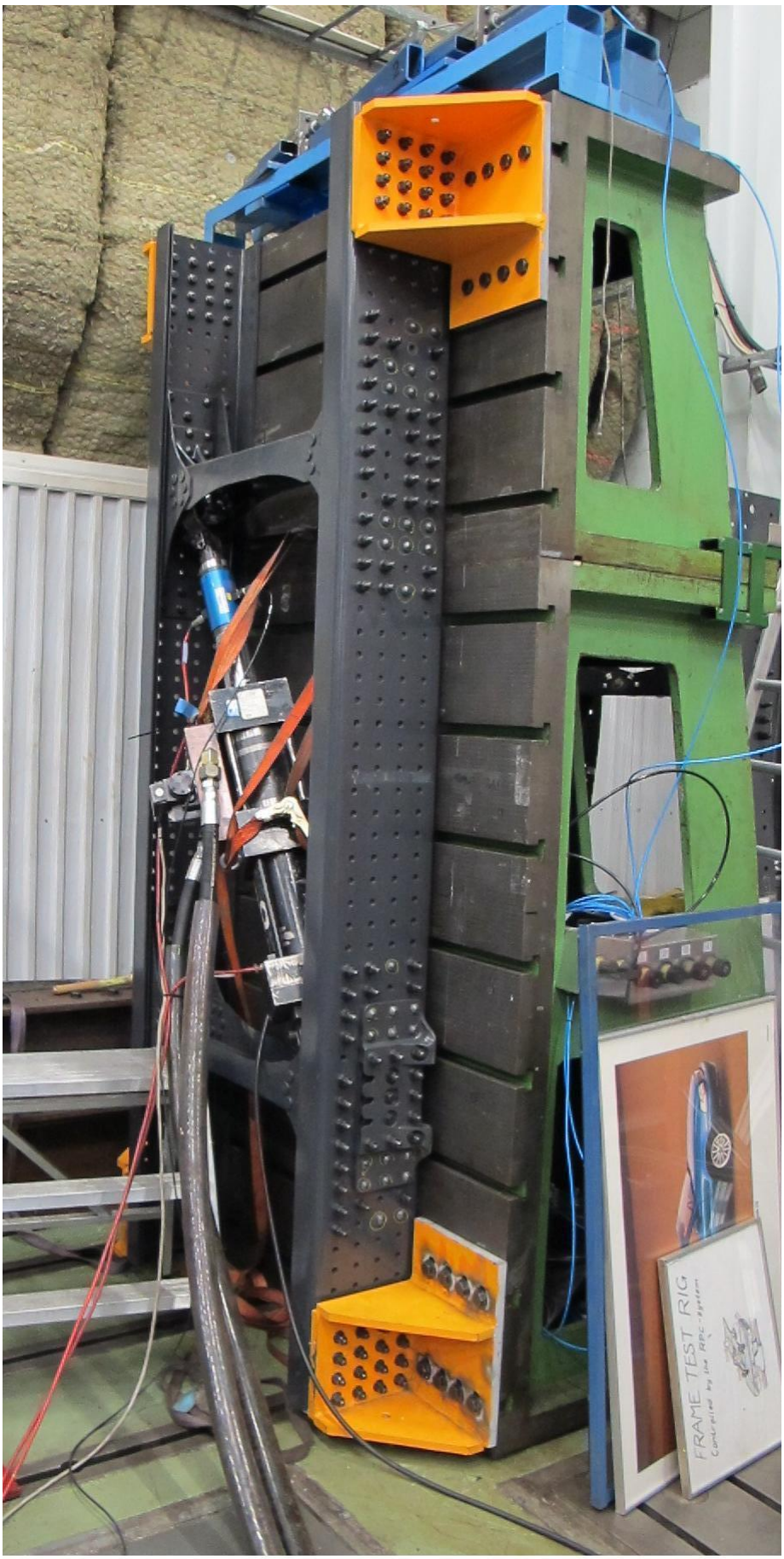

Figure B.5: Physical test rig

Appendix C

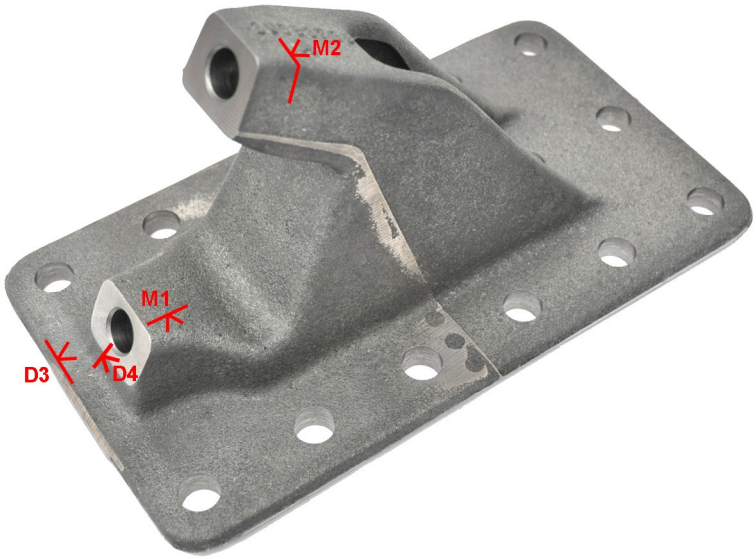

Figure C.1: Position of sample specimens

Table C.1: Material properties from a V-stay anchorage in 500-14

Specimen	Nodularity [%]	Nodule count [/mm^2]	Flake graphite rim depth [mm]	Amount pearlite [vol%]	Hardness [HBW]
M1	85	200	0	0	190±3
M2	87	190	0	0	192±2
D3	74	150	0	0	194±3
D4	81	180	0.2	0	188±2

Table C.2: Material properties from a V-stay anchorage in 500-7

Specimen	Nodularity [%]	Nodule count [/mm^2]	Flake graphite rim depth [mm]	Amount pearlite [vol%]	Hardness [HBW]
M1	90	280	0	40	190±1
M2	91	220	0	50	201±4
D3	88	210	0.25	40	204±2
D4	95	370	0	30	191±1